Environmental Earth Sciences (2019) 78:384
https://doi.org/10.1007/s12665-019-8385-y

ORIGINAL ARTICLE

Differentiating anthropogenic and natural sources of uranium by geochemical fingerprinting of groundwater at the Homestake uranium mill, Milan, New Mexico, USA

Johanna M. Blake[1] · **Philip Harte**[2] · **Kent Becher**[3]

Received: 9 July 2018 / Accepted: 22 June 2019

Abstract

A multiparameter geochemical-isotopic fingerprinting approach was used to differentiate anthropogenic and natural signatures of uranium contamination near the Homestake uranium mill site (Site), near Milan, New Mexico, USA. The Site consists of two tailings piles from milling operations and groundwater contamination from these tailings has been noted. The Site lies within the lower San Mateo Creek Basin and has multiple regional sources of uranium contamination from mining and mill operations. The Site is underlain by a heterogeneous alluvial aquifer, which is in turn underlain by basement rock of the Chinle Group aquifer and the underlying San Andres-Glorieta Formation aquifer. To help decipher signatures, several statistical approaches were used including principal component analysis, non-metric multidimensional scaling, and cluster analysis. Piper diagrams indicate two end-member water types at the Site, sulfate–Na–K generally in the Chinle Group aquifer and sulfate–Ca generally in the alluvial aquifer. There are wells from both aquifers that plot between the two end members. Uranium concentrations from the Site fall into three broad categories: less than the drinking water standard of 30 µg/L ($n=3$), from 30 to 100 µg/L ($n=9$), and greater than 100 µg/L ($n=8$). Component loadings in a principal component analysis are highest for uranium isotopes, uranium, molybdenum, chloride, sodium, ^{228}radium, and gross alpha–beta, which affect the similarities or differences among wells sampled. Results suggest that several alluvial wells north of the Site have groundwater with anthropogenic fingerprints from regional sources related to upgradient mining. Well water with higher uranium concentrations has uranium activity ratios close to 1, which is indicative of mining or milling signatures. These same wells have elevated radon activities. This information can be used to inform Site managers regarding the source of water related to uranium at the Site and provide an approach for geochemical fingerprinting.

Keywords Geochemical fingerprint · Uranium milling · Grants Mineral Belt · ^{234}U/^{238}U · Multivariate statistics

Introduction

Elevated concentrations of uranium (U) and co-occurring constituents, such as selenium (Se) and molybdenum (Mo), in groundwater at and surrounding the Homestake U mill site (Site) near Milan, New Mexico, USA, may originate from undisturbed ore deposits, mining activities, or milling activities from regional (within the San Mateo Creek Basin) or local (Site) sources (U.S. Environmental Protection Agency (EPA) 2011) (Fig. 1a, b). Dewatering of uranium mines in the San Mateo Creek mining district and the Ambrosia Lake mining district, both located in the San Mateo Creek Basin (Fig. 1a), led to contamination of downgradient sediment, alluvial aquifers, and deeper Chinle Group aquifers. Recharge to the deeper aquifers occurs via faults and subcropping of the Chinle Group strata beneath

Electronic supplementary material The online version of this article (https://doi.org/10.1007/s12665-019-8385-y) contains supplementary material, which is available to authorized users.

✉ Johanna M. Blake
jmtblake@usgs.gov

[1] U.S. Geological Survey, 6700 Edith Blvd. NE, Albuquerque, NM 87113, USA

[2] U.S. Geological Survey, 720 Gracern Rd, Columbia, SC 29210, USA

[3] U.S. Geological Survey, 501 W. Felix Street Bldg 24, Fort Worth, TX 76133, USA

Published online: 29 June 2019

EXPLANATION

Quaternary
Qa: Alluvium
Ql: Landslide
Qe: Eolian

Tertiary
Tnv/Tnr: Volcanics
Tmb: Tertiary Miocene basalts

Cretaceous
Kmf: Menefee Formation
Kpl/Kph: Point Lookout Sandstone
Km/Kmm/Kml: Mancos Shale
Kcc: Crevasse Canyon Formation
Kd/Kdm: Dakota Sandstone-Mancos Shale
Kg: Gallup Sandstone

Jurassic
Jm: Jurassic Morrison Formation
J: Jurassic undivided
Jsr: San Rafael Group

Triassic
Trc: Triassic Chinle Group

Permian
Psa: Permian San Andres Formation
P: Permian undivided

San Mateo Creek Basin
Fault trace
Mill and mine sites
Gaging stations

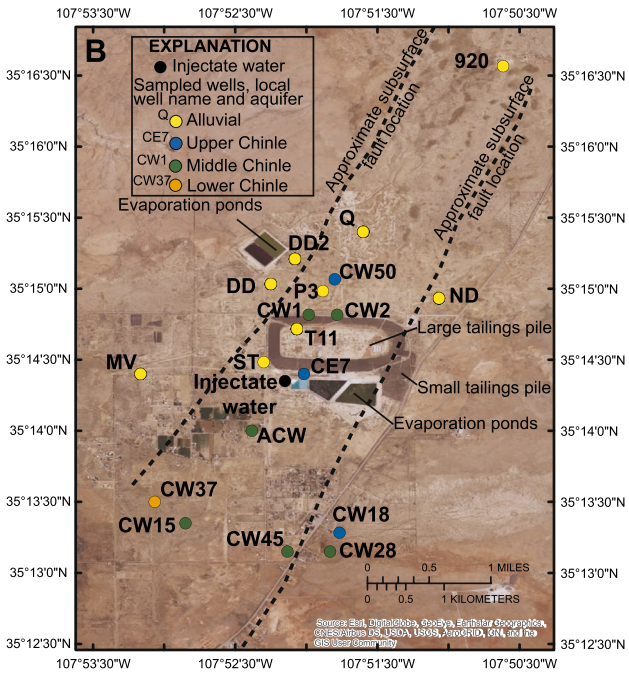

Homestake Mill within the San Mateo Creek Basin

Insert from A that is shown in B

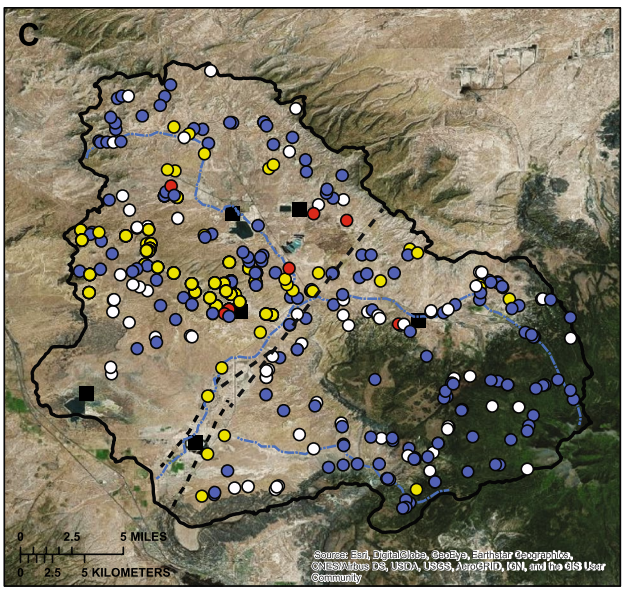

NURE Sediment Uranium Concentrations (mg/kg)

- 0.560-2.78
- 2.78-5.00
- 5.00-20.0
- 20.0-125

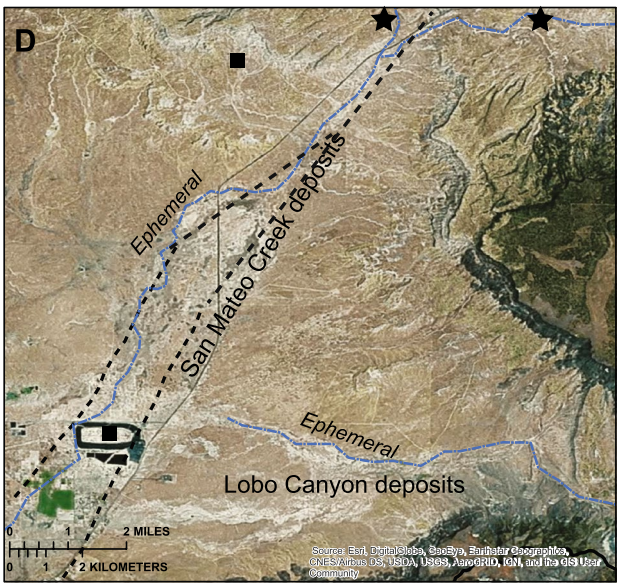

◂**Fig. 1** Map of the Site within New Mexico and the San Mateo Creek Basin. **a** Geology from NMBGMR (2003). **b** Aerial image of the Site with well spatial locations and formation type. **c** Aerial image of the San Mateo Creek Basin with NURE sediment concentration data. **d** Aerial image of the two main drainages into the Site, the San Mateo Creek and Lobo Canyon. Well names used in this study are those defined by the Site managers

the alluvium in the area (Gallaher and Goad 1981; Schoeppner 2008). The Chinle Group aquifers are near the surface in areas to the south and west of the Site and dip close to vertical beneath the alluvium. The alluvial aquifer was recharged as the mine water was discharged into natural waterways without treatment (Langman et al. 2012). In addition, there are two tailings piles, large and small (Fig. 1b), located on the Site, where infiltration or runoff may affect the water quality in underlying/adjacent aquifers. Uranium and Mo are considered the most mobile constituents of concern from U mill sites and Se is often associated with U ore (Morrison and Spangler 1992). Gallaher and Cary (1986) suggest that impacts of mine dewatering are evident by Mo concentrations in alluvial groundwater greater than 30 µg/L, U concentrations greater than 100 µg/L, changes in total dissolved solids (TDS), and changes in major water chemistry. Signatures of contaminants are evidenced by elevated concentrations in Mo, U, or Se at the near surface that decreases with depth. Selenium concentrations in sediments related to the Poison Canyon area are generally high (Gallaher and Cary 1986). The range of Se concentration in U ore in the Grants Mineral Belt, which includes the San Mateo Creek Basin, is 200–700 mg/kg (Brookins 1977).

Site cleanup standards are based on a local assessment of background concentrations of contaminants. The drinking water standard established by the EPA for U is 30 µg/L (EPA 2017). Groundwater samples categorized as background samples for this Site had levels of U exceeding this drinking water standard (Homestake Mining Company and Hydro-Engineering, LLC 2014). Uranium concentrations in the background samples were likely affected by pervasive mining activities in the basins upgradient of the mill site, and there is potential for regional contamination to impact local water quality (Homestake Mining Company and Hydro-Engineering, LLC 2014). Regional U concentrations in groundwater from the San Mateo Creek Basin were measured from < 10 to 500 µg/L (New Mexico Environment Department, NMED 2012). Based on the background data, the EPA, NMED, and the Nuclear Regulatory Commission set the cleanup standard of U at 160 µg/L in the alluvial aquifer (Agency for Toxic Substances and Disease Registry, ATSDR 2009; Homestake Mining Company and Hydro-Engineering, LLC 2014). Because groundwater recharges from the alluvium to the underlying Chinle Group aquifer through subcropping strata, a similar standard is being applied to parts of the Chinle Group (Homestake Mining Company and Hydro-Engineering, LLC 2004). The areas of the Chinle Group aquifer in which the chemical composition of water has been altered by inflow of alluvial water are designated as the mixing zone, and have a cleanup standard of 160 µg/L U; parts of the formation in which the chemical composition of water has not been altered by inflow of alluvial water are designated as the non-mixing zone and have a different cleanup standard (Homestake Mining Company and Hydro-Engineering, LLC 2004).

The main objective of this paper is to differentiate the water type and source of U in groundwater in wells at and near the Site as either (1) sourced regionally from upgradient mining, (2) sourced locally by the mill Site, (3) sourced from deeper groundwater from the Chinle Group aquifer, and (4) sourced through other mechanisms such as upwelling from faults or mobility from surficial sediments. Water type and U source were determined using a geochemical fingerprinting approach of well-to-well variability and end-member variability. Multiple lines of evidence, including general chemistry, stable isotopes, radiogenic isotopes, borehole geophysics, groundwater age dating, and multivariate statistics were used to differentiate sources of water and specifically sources of U in the groundwater.

Geological setting and site description

The geology, hydrogeology, and hydrogeochemistry in the area are complex (Langman et al. 2012; Gallaher and Goad 1981). Numerous faults near the Site may affect the groundwater hydrogeology and geochemical interactions. In addition, the Chinle Group hydrogeologic units subcrop south of the Site (Fig. 2). Passive sampling of select wells in the area combined with spectral gamma-ray results indicate that alluvial aquifer stratigraphy and long screens in the monitoring wells play a role in degree of mixing in each well (Harte et al. 2019). The complexities of the site require rigorous analysis afforded by statistical techniques and multiple lines of evidence.

The Grants Mineral Belt is a southeast-trending zone of U deposits along the southern margin of the San Juan Basin in New Mexico (Brookins 1977). There are several mine and mill locations within the San Mateo Creek Basin, where the Site is located (Fig. 1a). The Site, north of Milan, New Mexico in the lower San Mateo Creek Basin, opened in 1958 and closed in 1990 (ATSDR 2009). The mill operations used an alkaline leach–caustic precipitation process to concentrate U from the ores (ATSDR 2009), using sodium carbonate and sodium bicarbonate (Nuclear Regulatory Commission 1981). Currently (2019), there are large and small tailings piles from mill processing and several evaporation ponds at the Site (Fig. 1b). As previously mentioned, these tailings sit atop an alluvial aquifer, which is underlain by the Upper, Middle, and Lower Chinle Group aquifers. Well names used

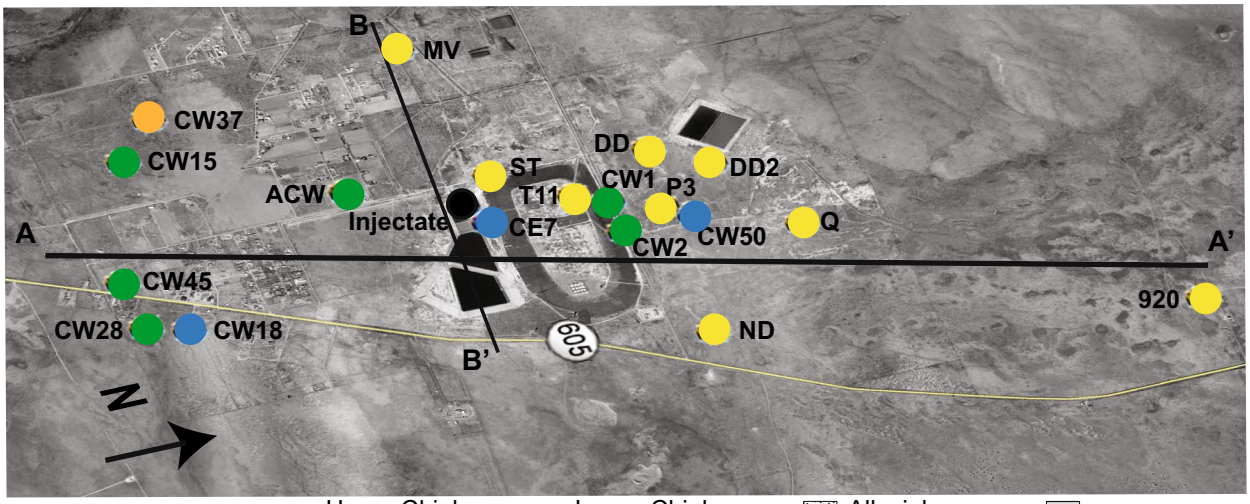

Injectate Well
Alluvial aquifer Well
Upper Chinle Aquifer Well
Middle Chinle Aquifer Well
Lower Chinle Aquifer Well
Alluvial aquifer
Chinle Shale
Chinle Sandstone

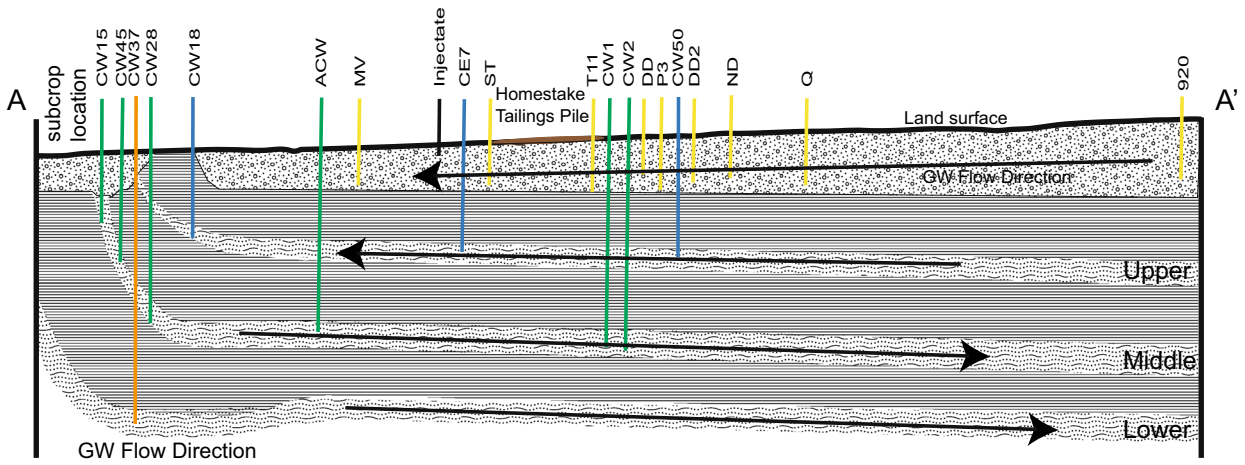

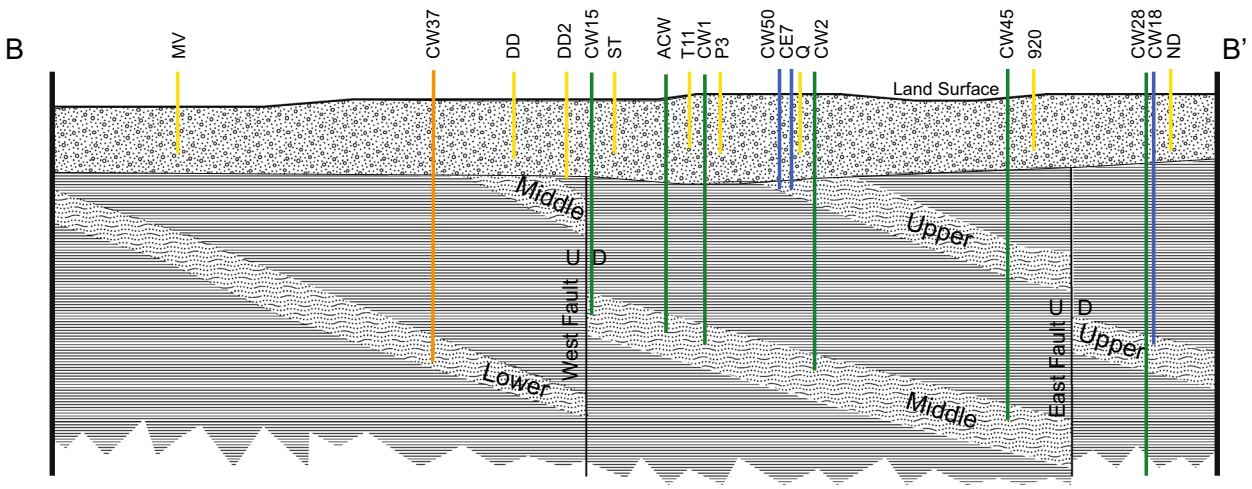

Conceptual models- not to scale

◂**Fig. 2** Aerial image of the Site with well spatial locations, formation of completion, and cross-sectional locations. Cross sections A–A′ and B–B′ are shown below the aerial image. Arrows show the general direction of groundwater flow. The subcrops of the Chinle Group are shown in cross section A–A′. All figures are conceptual and based upon information presented in Hydro-Engineering LLC (2001) and Homestake Mining Company and Hydro-Engineering, LLC (2004)

in this study are those defined by the Site managers. Alluvial aquifer wells have the simplest alphabetic names and Chinle Group aquifer wells start with CW or CE (Fig. 1b).

The arroyo and ephemeral stream channels in the area are Quaternary (Holocene) alluvium with sand, gravel, and silt/clay in and adjacent to modern arroyo channels. The alluvium is generally 0–10 m thick and at or near the grade of modern channels (Cather 2011). Adjacent eolian and alluvial deposits from the Upper Pleistocene–Holocene, which are older than the arroyo and ephemeral stream deposits, have surface expression near the Site, likely because of uplift and erosion over geologic time. These older deposits of eolian sand and loessic silt are 0–10 m thick and have been locally reworked by alluvial processes (Cather 2011). The San Mateo Creek sediments are younger than the underlying eolian and alluvial deposits and may affect groundwater flow and geochemical processes based on the sediment sorting, grain size, mineralogy and chemical composition. For example, where sediments are coarse, groundwater flow is enhanced, and groundwater tends to be oxic (Turner-Peterson and Fishman 1986; Brookins 1977). In contrast, in finer grained sediment, groundwater flow rates are slow and water may be chemically reducing, which can affect mobility of redox-sensitive chemical elements such as U and Se (Turner-Peterson and Fishman 1986; Brookins 1977).

Sources of uranium at the site

Surface sediments collected in the 1970s through a program called the National Uranium Resource Evaluation (NURE) (U.S. Geological Survey, USGS 2004) show the distribution of U in soil samples and stream sediments in the San Mateo Creek Basin (Fig. 1c). Based on the NURE data, the ranges of soil and sediment U concentrations in four groupings are (1) the lowest concentration reported to the crustal average of 2.78 mg/kg (EPA 2008); (2) > 2.78 mg/kg to 5.00 mg/kg; (3) > 5.00 mg/kg to 20.0 mg/kg; and (4) > 20.0 mg/kg and 125 mg/kg. The highest concentrations of U in sediment are found near the San Mateo Creek, Ambrosia Lake, and Poison Canyon mines (Fig. 1a, c). Concentrations of U in sediments in Lobo Creek are generally lower than concentrations in San Mateo Creek and Arroyo del Puerto (Fig. 1a, c, d). These channels, Lobo Creek, San Mateo Creek, and Arroyo del Puerto, flow towards the Site and may affect the chemistry of sediments and water near the Site. The confluence of San Mateo Creek and Arroyo del Puerto, both ephemeral creeks, lies in the upper San Mateo Creek Basin north of the Site (Langman et al. 2012). From the confluence, San Mateo Creek traverses southwest directly towards the Site (Fig. 1a, d). Over 30 years ago, the San Mateo Creek channel course was changed by Homestake Mining Company to flow to the west of the Site (Roca Honda Resources, LLC 2011); however, there is still a surface expression of the original channel in sediments from northeast to southwest to the north of the Site (Fig. 1d).

During active mining, mine discharge from Ambrosia Lake and San Mateo mines was directed into San Mateo Creek and Arroyo del Puerto; these ephemeral streams became perennial while mine discharge continued (Kaufman et al. 1976). There is evidence that groundwater in the area rose as much as 15 m (50 feet) from 1950 to 1980, then declined when mine discharge to the channels stopped (Weston Solutions, Inc. 2016). USGS streamgaging stations recorded discharge in the San Mateo Creek (1977–1982) and Arroyo del Puerto channels (1979–1982) above their confluence (USGS 2018) (Figure S1). Water from these channels may have infiltrated into shallow alluvial aquifers or evaporated, leaving behind constituents of concern such as U, Se, and radionuclides adsorbed or precipitated on alluvial sediments. Constituents in water that recharged the alluvial aquifer could be mobile under geochemical conditions appropriate for each constituent (NMED 2008). On the land surface, streambed sediments containing sorbed or precipitated constituents could be scoured and mobilized during larger storm events. Storm runoff could transport sediments containing mine water constituents downstream where they could be redeposited as stormflow recedes (Gallaher and Cary 1986). This process can readily occur during sporadic high-intensity rain events that occur during the summer monsoon season characteristic to this geographic area (Blake et al. 2017a).

Under current conditions, the San Mateo Creek and Arroyo del Puerto are ephemeral and further downstream, the Rio San Jose near Grants, NM, is perennial (Figure S1) (Roca Honda Resources, LLC 2011). The San Mateo Creek channel widens below the confluence with the Arroyo del Puerto, the slope of the channel decreases, and flow rarely reaches as far as a few miles past the confluence with Arroyo del Puerto (Roca Honda Resources, LLC 2011).

Water moves through the alluvium and Upper Chinle Group from northeast to southwest in the study area (Baldwin and Anderholm 1992). The general direction of flow in the Middle and Lower Chinle Group aquifers is from southwest to east and northeast and flow is downdip (Langman et al. 2012) (Fig. 2). The dip of the Chinle Group aquifer is approximately to the north.

The Chinle Group is typically a confining unit in the area, with hydraulic conductivity values of the shale layers in the Chinle Group ranging from 10^{-1} to 10^{-8} ft/day (Baldwin

and Anderholm 1992; Baldwin and Rankin 1995). However, in between the shale layers are three layers of more coarse-grained deposits. In general, recharge to the Chinle Group aquifer is from downward leakage of water in the formation and can occur at subcrop locations (Fig. 2) (Baldwin and Anderholm 1992). There are two subsurface faults that cross the study area (Cather 2011) (Figs. 1b, d, 2). The Chinle Group aquifers are intersected by these faults that bound the overlying area of the large tailings pile. Along fault traces, permeability may be higher than in other areas (Fetter 2001), depending upon the material in the fault zone (Langman et al. 2012), resulting in a conduit for mixing between the alluvial and Chinle Group aquifers (ATSDR 2009). Groundwater mounding below the large tailings pile because of treated water injection has been reported (Homestake Mining Company of California 2012); however, the present study did not focus on groundwater levels, but rather geochemical signatures of the groundwater.

Controls on uranium mobility

Uranium mobility is affected by redox, pH, and aqueous complexes. The insoluble form U(IV) is predominant in U ore (Brookins 1977; Hall et al. 2017) and can be oxidized in the presence of molecular oxygen or nitrate, among other constituents (Borch et al. 2010; Van Berk and Fu 2017). Once U(IV) solids are exposed to oxygen and oxidized during mining or milling, the oxidation state becomes U(VI) (Basu et al. 2015), which is mobile in water. In addition, abiotic and biotic nitrate reduction (denitrification) reactions may produce intermediates such as nitrite and nitrous oxide that will abiotically oxidize U(IV) to U(VI) (Nolan and Weber 2015; Senko et al. 2002). Microbial denitrification can be identified with stable isotopes of nitrogen and oxygen, where δ^{18}O-nitrate vs δ^{15}N-nitrate has a linear relation and high positive slope (Basu et al. 2015; Bottcher et al. 1990).

The dominant form of U adsorbed to sediments under oxidizing conditions is the uranyl ion, $(UO_2)^{2+}$ (Alam and Cheng 2014). In the presence of high carbonate concentrations in water and at pH of 6 and higher (Dong and Brooks 2006), uranyl ion–calcium–carbonate aqueous complexes are formed, which mobilizes U(VI) from sediments into water (Leavitt et al. 2011; Briganti et al. 2017). These reactions governing U mobility are potential transport and distribution pathways of U as a contaminant of concern.

Geochemical fingerprints

Geochemical constituents in groundwater that has recharged from the surface evolve due to interaction with rocks and sediments along the groundwater flow path. Geochemical fingerprints expressed as major ion composition, U isotope ratios (^{234}U/^{238}U), radium isotopes (^{226}Ra and ^{228}Ra), radon concentrations (Rn), sulfur isotopes (δ^{34}S), and stable isotopes of water [oxygen (δ^{18}O) and hydrogen (δD)] can help to understand the type of water and source of U in groundwater (Basu et al. 2015; Yabusaki et al. 2007; Christensen et al. 2004; Zielinski et al. 1997).

The U activity ratio (UAR) of ^{234}U/^{238}U can indicate the origin of groundwater (Kamp and Morrison 2014). The ^{234}U isotope is a daughter of the ^{238}U isotope and when the UAR is equal to 1, the isotopes have reached secular equilibrium, and the activities are equal. U isotopes reach secular equilibrium in approximately 1 million years. Because the ore deposits in the area are older than 1 million years, the ore bodies are likely in secular equilibrium, and water with U derived from contact with mine tailings or mill sites should have a UAR equal to 1 (Corcho et al. 2015). The UAR of two discharge effluent samples collected in 1990 from the San Mateo Mine are reported as 1.06 and 1.07 (Van Metre et al. 1997). Additionally, the milling process completely dissolves the U ore minerals, which results in a theoretical UAR value of around 1–1.3 in the groundwater affected by the milling (Kamp and Morrison 2014). A UAR greater than 1 may indicate water unaffected by mine or mill tailings. For example, the UAR from samples in bedrock wells of the Dakota and Morrison Formations, thought to be unaffected by mining in the area, ranged from 2.0 to 6.7 (Van Metre et al. 1997).

Radium (Ra) isotopes and radon (Rn) concentrations in groundwater can indicate interaction with material from mines or mills. For instance, ^{226}Ra (a daughter product of radioactive decay of ^{238}U) concentrations tend to increase near ore bodies (Kaufman et al. 1976). Natural background concentrations of ^{226}Ra in the area are generally around 3 picocurie per liter (pCi/L), whereas the effluent from operating mines in the Grants Mineral Belt had ^{226}Ra concentrations of 100 pCi/L or more (Kaufman et al. 1976). Seepage from the large tailings pile had a ^{226}Ra concentration of 52 pCi/L (Kaufman et al. 1976). The range of Rn concentrations from groundwater percolating through U ore bodies can range from 2300 pCi/L to 109,000 pCi/L depending on the source of the water (Sahu et al. 2016). The Rn concentration in water can be diluted with increasing distance from the ore body (Sahu et al. 2016); however, because Rn has a half-life of 3.8 days, it does not persist far from its source and the dilution effect may be negligible.

Sulfate is a major constituent related to mine waste and mill tailings (Abdelouas 2006; Ries 1982). To differentiate between natural sulfate concentrations and concentrations related to mining or milling, stable sulfur isotopes of sulfate can be analyzed to identify the source of the sulfate (Kamp and Morrison 2014; Ries 1982). For example, δ^{34}S of sulfate values in groundwater surrounding the mill site located in

the Ambrosia Lake mining district range from −28.5 per mil (‰) to +10.4‰ (Ries 1982). Pyrite in sandstone-type U deposits in the Grants Mineral Belt has a $\delta^{34}S$ range of −27‰ to −1.8‰ (Jensen 1963). For the Faith Mine ore, located in Poison Canyon, $\delta^{34}S$ is equal to −27.2‰ and the $\delta^{34}S$ range identified from water in tailings ponds and groundwater near U mill sites in the Grants Mineral Belt and Navajo Nation is −5‰ to 5‰ (Kamp and Morrison 2014).

As relatively conservative isotopes, isotopic ratios of oxygen ($\delta^{18}O$) and hydrogen (δD) are not altered on contact with organic or geologic materials (Kendall and Caldwell 1998), which make them good chemical tracers of recharged water. However, the isotopes are affected by mass-dependent fractionation, which manifests as differences in physical and chemical properties based on the mass differences (Kendall and Caldwell 1998). These differences are related to temperature changes during precipitation and evaporation of water (Ingraham 1998) and occur during atmospheric exposure. Once precipitation enters the ground beyond the zone of evaporation, the isotopic signature is fixed. Stable isotopes δD and $\delta^{18}O$ can be indicative of recharge temperatures, evaporation, or upwelling from deep aquifers (Ingraham 1998; Robertson et al. 2016).

Conceptualization of U sources

Identifying the source of U at a site can be complex, especially in a location with multiple potential anthropogenic and natural sources. At this Site, there are four water sources defined: (1) regionally sourced from mining to the north of the Site; (2) locally sourced by the mill Site; (3) sourced from a deeper aquifer; and (4) other. Within each source, there is the potential for regional and local differences including contaminated and uncontaminated wells, natural heterogeneity, and differences in aquifers. The variability among the individual wells may be associated with the lithology, hydrogeology, or spatial location, which may be seen in Figs. 1 and 2. The specific geochemical signatures of each well were used to understand the general source water. Statistical analyses were used to narrow down the most appropriate geochemical signatures for this Site. Table 1 identifies the geochemical signature, description of the results that aid in identifying water source and relation to mining, and the associated figure in the text. In some cases, there may be more than one water source to a well.

Methods

Groundwater samples were collected from twenty wells both distal and proximal to the Site for an array of chemical constituents (Figs. 1b, 2; Blake et al. 2017b; Harte et al. 2018b) to help delineate chemical signatures associated with the water sources in the area. A combination of monitoring wells, existing remedial extraction wells, and residential wells was sampled. Wells are screened in alluvium and in the Upper, Middle, and Lower Chinle Group aquifers. The injectate is water pumped from the tailings pile, treated in the reverse osmosis plant at the Site, and mixed with water from the San Andres-Glorieta Formation aquifer prior to injecting into the subsurface (Homestake Mining Company and Hydro-Engineering, LLC 2014) (injectate; Figs. 1b, 2). Groundwater-quality sampling followed volumetric purging procedures as outlined in the USGS National Field Manual (USGS 2006). Details of sampling, collection, preservation techniques, and chemical analyses are included in the Supplementary Information (SI).

Three multivariate statistical techniques, principal component analysis (PCA), non-metric multidimensional scaling (NMDS), and cluster analysis were used to quantitatively investigate the similarities and differences in groundwater geochemistry in the wells (de Carvalho Filho et al. 2017; Jiang et al. 2015). Details of these techniques are included in the SI.

For this study, the following constituents were used as input for the PCA, NMDS, and cluster analysis: gross alpha, gross beta, ^{226}Ra, ^{228}Ra, ^{234}U, ^{238}U, uranium concentrations, alkalinity, calcium, iron, magnesium, chloride, sulfate, sodium, molybdenum, and vanadium. These constituents were chosen based on the component loadings calculated from PCA when using all measured constituents. The constituents chosen had at least a 0.8 component loading when compared with all measured constituents.

Piper diagrams were created using GWChart (USGS 2015). Geochemical modeling to determine aqueous complexes and mineral saturation indices was completed in PHREEQC version 3.4.0.12927 using the minteqv4 database (Parkhurst and Appelo 1999). Major and trace element chemistry data of filtered water from each well were used as input for the model and are accessible in the corresponding data release (Blake et al. 2017b). Groundwater ages based on dating of well samples were used to calculate groundwater travel times at the Site. Details are given in the SI.

Results and discussion

Each section of the results and discussion describes the line of evidence used to identify the source of U to each well. Groups of wells with similar signatures are discussed.

Major water types

Two dominant end members in waters from the wells sampled in this study, sulfate–calcium (SO_4–Ca) and sulfate–sodium plus potassium (SO_4–Na + K), are identified in

Table 1 Geochemical signature and water source descriptions

Water source	Piper diagram (Fig. 3)	Co-constituents (Fig. 4 and S2)	PCA (Fig. 6a,b)	NMDS (Fig. 6c)	Cluster (Fig. 6d)	$^{234}U/^{238}U$ (Fig. 7a)	Radon (Fig. 7b)	Radium (Fig. 7c)	Gross alpha/beta (Fig. 7d)
1. Regionally sourced from upgradient mining	Wells that near each other have similar water types. End members and wells mixed between end members can be identified	Higher U concentration, likely closer to source. High TDS may indicate mining or mill source	Wells that plot near each other may have the same or similar water sources	Wells that plot near each other may have the same or similar water sources	Wells that plot near each other may have the same or similar water sources	UAR = 1, mining or mill tailings signature. UAR > 1.3 may not be affected by mining or mill tailings. UAR between 1 and 1.3 may show mixing	High radon may be associated with inputs from faults or proximity to uranium source	High Ra concentrations may indicate proximity to source	High Gross Alpha may show wells with radioactive sediments
1a. San Mateo Creek Channel (Fig. 1d): wells within the channel may be affected by mine discharge and adsorption or precipitation on sediments	Wells that near each other have similar water types. End members and wells mixed between end member can be identified	Higher U concentration, likely closer to source. High TDS may indicate mining or mill source	Wells that plot near each other may have the same or similar water sources	Wells that plot near each other may have the same or similar water sources	Wells that plot near each other may have the same or similar water sources	UAR = 1, mining or mill tailings signature. UAR > 1.3 may not be affected by mining or mill tailings. UAR between 1 and 1.3 may show mixing	High radon may be associated with inputs from faults or proximity to uranium source	High Ra concentrations may indicate proximity to source	High Gross Alpha may show wells with radioactive sediments
2. Locally sourced by the mill Site	Wells that near each other have similar water types. End members and wells mixed between end members can be identified	The subcrop area may allow for mixing from the Site to the Chinle Group aquifer	Wells that plot near each other may have the same or similar water sources	Wells that plot near each other may have the same or similar water sources	Wells that plot near each other may have the same or similar water sources	UAR = 1, mining or mill tailings signature. UAR > 1.3 may not be affected by mining or mill tailings. UAR between 1 and 1.3 may show mixing	High radon may be associated with inputs from faults or proximity to uranium source	High Ra concentrations may indicate proximity to source	High Gross Alpha may show wells with radioactive sediments
3. Sourced from deeper aquifer groundwater	Wells that plot near each other have similar water types. End members and wells mixed between end members can be identified	The subcrop area may allow for mixing from the Site to the Chinle Group aquifer	Wells that plot near each other may have the same or similar water sources	Wells that plot near each other may have the same or similar water sources	Wells that plot near each other may have the same or similar water sources		High radon may be associated with inputs from faults or proximity to uranium source		Not a clear indicator of U source

Table 1 (continued)

Water source	Piper diagram (Fig. 3)	Co-constituents (Fig. 4 and S2)	PCA (Fig. 6a,b)	NMDS (Fig. 6c)	Cluster (Fig. 6d)	$^{234}U/^{238}U$ (Fig. 7a)	Radon (Fig. 7b)	Radium (Fig. 7c)	Gross alpha/beta (Fig. 7d)
3a. Near fault (Fig. 1b): wells close to the faults may have upwelling of water from deeper groundwater	Wells that plot near each other have similar water types. End members and wells mixed between end members can be identified	The subcrop area may allow for mixing from the Site to the Chinle Group aquifer	Wells that plot near each other may have the same or similar water sources	Wells that plot near each other may have the same or similar water sources	Wells that plot near each other may have the same or similar water sources		High radon may be associated with inputs from faults or proximity to uranium source		Not a clear indicator of U source
3b. Near Subcrop (Fig. 2): potential for mixing between alluvial and Chinle aquifers	Wells that plot near each other have similar water types. End members and wells mixed between end members can be identified	The subcrop area may allow for mixing from the Site to the Chinle Group aquifer	Wells that plot near each other may have the same or similar water sources	Wells that plot near each other may have the same or similar water sources	Wells that plot near each other may have the same or similar water sources		High radon may be associated with inputs from faults or proximity to uranium source		Not a clear indicator of U source
4. Other sources	Well fits more than one category or final category is unclear	Well fits more than one category or final category is unclear	Well fits more than one category or final category is unclear	Well fits more than one category or final category is unclear	Well fits more than one category or final category is unclear	UAR = 1, mining or mill tailings signature. UAR > 1.3 may not be affected by mining or mill tailings. UAR between 1 and 1.3 may show mixing	Well fits more than one category or final category is unclear	Well fits more than one category or final category is unclear	not a clear indicator of U source

Each geochemical signature was used to interpret the source of water to individual wells

PCA principal components analysis, *NMDS* non-metric multidimensional scaling

the Piper diagram (Fig. 3). End member 1, SO_4–Ca, is similar to mine water discharge from the Arroyo Puerto Mine in the Ambrosia Lake mining district (Gallaher and Cary 1986). The alluvial aquifer wells DD, DD2, P3, 920, and Q plot in this area. These wells are within the San Mateo Creek channel and may indicate an influence from a water source to the north.

End member 2, SO_4–Na + K, is more dominant in groundwater from the Middle Chinle Group aquifer than from the alluvium at the Site. However, groundwater from the large tailings pile (well T11) also plots in end member 2. This may confirm that well T11 is drilled into the Chinle Group aquifer. Mine waters in the Grants Mineral Belt can contain higher concentrations of sodium and sulfate compared to natural waters (NMED 2008), which may account for the higher values of these constituents in well T11. Na–SO_4–Cl groundwater is commonly created by dissolution of evaporite minerals such as gypsum ($CaSO_4$) and halite (NaCl) (Vengosh 2003); evaporite dissolution could influence the composition of end member 2 groundwater samples. The Chinle Group is known to have gypsum deposits in some locations (Cather 2011), and the aridity of the region may cause evaporite or salt deposits in the alluvium. Evaporite crystals have been observed in sediments along the Rio San Jose, which flows through the Grants Mineral Belt (Popp et al. 1983). Wells that plot between the two end members in Fig. 3 vary in aquifer type and spatial location, which further demonstrates the complexity of groundwater source and composition in wells at this site.

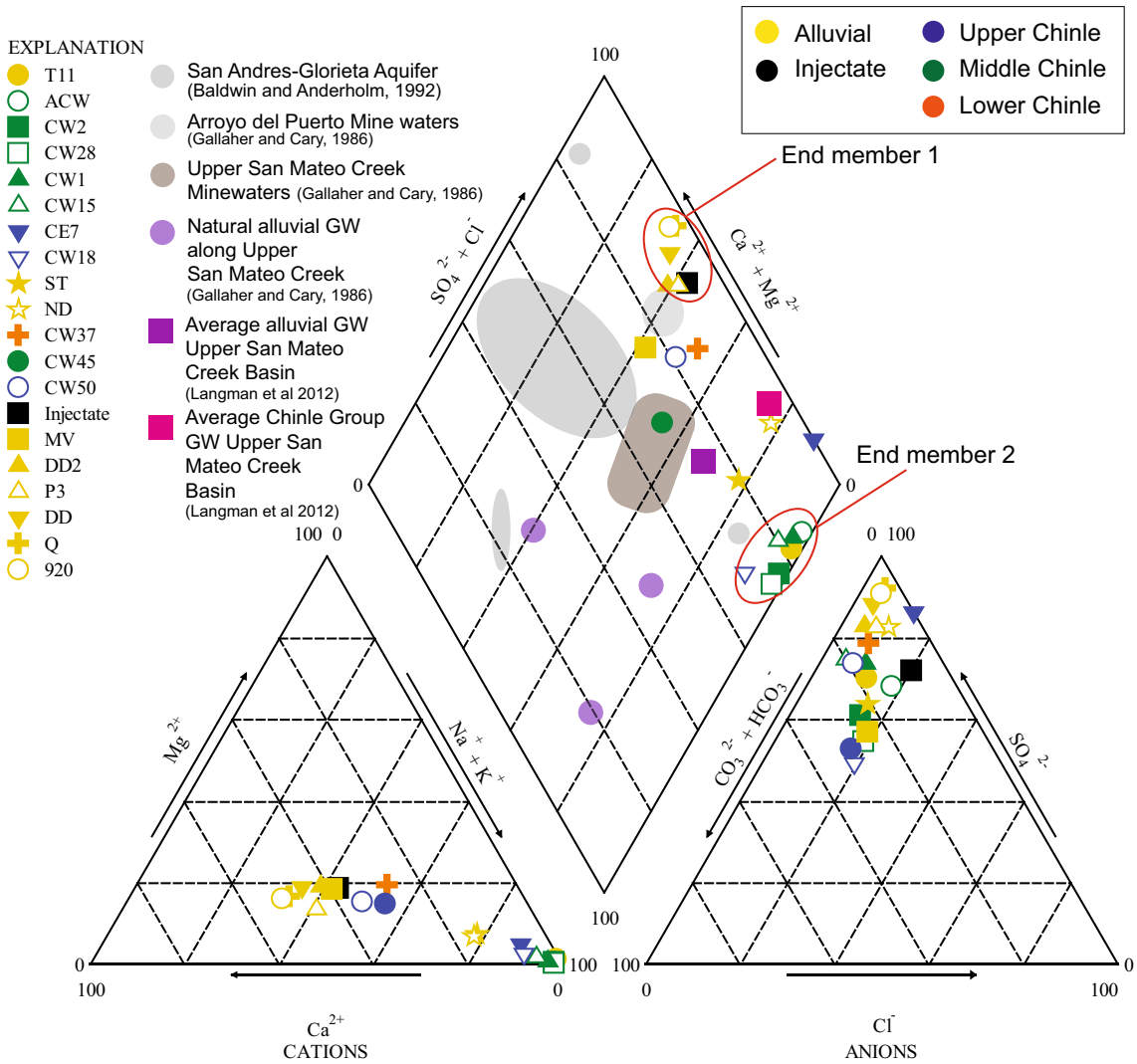

Fig. 3 Piper diagram of groundwater chemistry from wells sampled for this study. Regional groundwater data are included for comparison

Uranium, selenium, and molybdenum concentrations in groundwater

Uranium concentrations in water samples from the Site fall into three broad categories: (1) less than the drinking water standard of 30 µg/L ($n=3$), (2) from 30 to 100 µg/L ($n=9$), and (3) greater than 100 µg/L ($n=8$). Uranium concentrations in groundwater collected from the Site range from 25.0 to 22,700 µg/L (Fig. 4a, b) as reported in Harte et al. (2018a). The three highest dissolved U concentrations were measured in wells within and directly south of the large tailings pile [Chinle Group aquifer: CE7 (22,700 µg/L), Alluvial aquifer: T11 (10,029 µg/L), and ST (2709 µg/L)] and the three lowest U concentrations were measured in ND (25.0 µg/L), P3 (26.0 µg/L), and CW18 (28.0 µg/L), which are not spatially adjacent to each other. The higher U concentrations in CE7, T11, and ST were expected based on historical data and proximity to the U milling operations. Alluvial wells 920, DD2, DD, T11, MV, ST, and Chinle Group wells CE7 and CW45 have U concentrations greater than 100 µg/L, which could indicate a source from mining or milling. Given the proximity of alluvial wells 920, DD2, DD, and MV to the San Mateo Creek channel (Fig. 1a, b), these U concentrations may indicate an effect from mine dewatering. The dewatered mine water recharged the alluvium north of the Site from the upper San Mateo basin. Sediments transported in the San Mateo Creek channel from north to south contained potentially higher U source concentrations. If the dewatered mine water encountered subsurface reducing conditions, U would precipitate out of solution, and could serve as a source of U if exposed to oxic conditions. Wells T11, ST, and CE7 are adjacent to the tailings pile and water in these wells may be affected by activities at the Site. Water from well CW45 may reflect mixing with the alluvial aquifer due to its proximity to the subcrop area (Fig. 2).

Well DD (U = 103 µg/L), which is spatially adjacent to well DD2, has a U concentration less than half of the concentration of DD2 (U = 250 µg/L). The western fault at the Site is closer to DD2 than to DD (Figs. 1b, 2), and upwelled water from the fault may contribute to water in DD2. Well DD2 is drilled approximately 3 m (10 ft) into the upper Chinle Group Shale and is partially screened in the Chinle Group Shale. Wells DD and DD2 are adjacent to the western evaporation ponds, which may have an effect on the U concentrations in these wells, although leakage was not considered because the evaporation pond was reported to be lined (Homestake Mining Company and Hydro-Engineering, LLC 2014). Further evaluation of leakage from the evaporation pond may be beneficial.

The concentration of Se and Mo vary among the wells. The EPA drinking water standard for selenium is 50 µg/L and the highest concentration of Se was in well CE7 (900 µg/L; Fig. 4a, c). Wells Q, P3, and 920 (Fig. 4a, c) also had elevated Se concentrations (470, 300, and 290 µg/L, respectively). Selenium concentrations in sediments related to the Poison Canyon area are generally high (Gallaher and Cary 1986), and these sediments could be the source of elevated Se in the wells upgradient from the Site. The average Se concentration in discharge to the San Mateo Creek drainage from the Ambrosia Lake Mining District was 240 µg/L (Gallaher and Cary 1986). Well DD has a Se concentration 33 times higher than that found in well DD2. This result may be explained by proximity to Poison Canyon, mixing from the middle Chinle Group aquifer waters, and/or mixing with groundwater from the nearby fault.

Wells CE7, T11 and ST have the highest concentrations of Mo, at 28,000, 22,000, and 3500 µg/L, respectively, which follows the same pattern as the elevated U concentrations (Fig. 4b, c) and may be explained by the fact that U and Mo are often the most mobile elements associated with U mills (Morrison and Spangler 1992). Well CW18 may have a different source of the elevated Mo due to the higher concentration compared to nearby wells.

In addition to U or Mo concentrations, total dissolved solids (TDS) may be indicative of U source water or mixed water. For instance, the average TDS concentration in alluvial groundwater upgradient of the San Mateo Creek mine was 400 mg/L (Brod and Stone 1981) and the average TDS in alluvial groundwater north of Arroyo del Puerto, in the Ambrosia Lake mining area, was 5900 mg/L (Brod and Stone 1981). Additionally, the average TDS concentration in alluvial groundwater below the confluence of Arroyo del Puerto and San Mateo Creek was 2000 mg/L (Kaufman et al. 1976) (Figure S2). The TDS concentrations from the alluvial wells sampled for this study range from 2000 mg/L (ND) to 7500 mg/L (T11). Wells MV, P3, 920, DD2, and Q have concentrations between 2000 and 3000 mg/L and wells DD and ST both have TDS concentrations of 3700 mg/L (Figure S2). These results suggest that wells north of the Site may have mine discharge water associated with them. The similarity of TDS in groundwater from well DD and ST may suggest that well DD has water from the upgradient evaporation pond seeping into the groundwater or water from the large tailings pile being transported in groundwater to the well.

Uranium mobility

Geochemical modeling

Geochemical modeling results show that the dominant species of U in the groundwater of the sampled wells is U(VI), which is typical of the species related to surface mining and milling activities. The dominant aqueous complex is a uranyl carbonate, which suggests that U in groundwater is mobile. However, the presence of hydrous ferric oxides (HFO) in sediments can increase the sorption of U to

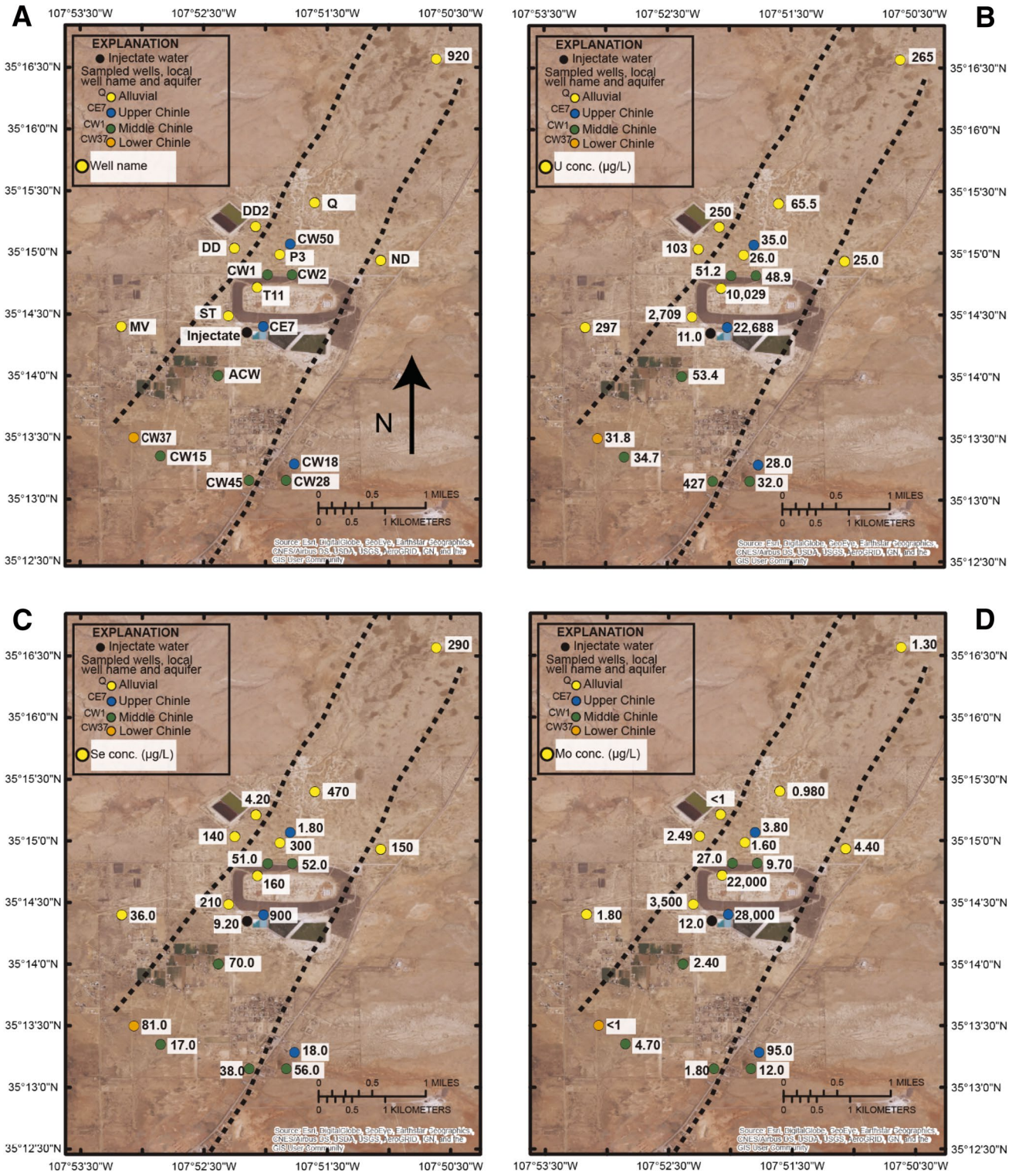

Fig. 4 Aerial photos of Site with **a** well names, **b** uranium concentrations, **c** selenium concentrations, and **d** molybdenum concentrations measured in each well at the time of sampling

sediments (Johnson et al. 2016). Harte et al. (2019) reports U spectral gamma spikes in some red clays at the Site, which are likely associated with HFOs. Water in all the samples were supersaturated with respect to the HFOs ferrihydrite ($(Fe^{3+})_2O_3 \cdot 0.5H_2O$), goethite (FeO(OH)), and lepidocrocite (γ-FeO(OH)).

Nitrogen isotopes and redox

The comparison of δ^{18}O-nitrate vs. δ^{15}N-nitrate for the alluvial groundwater and Chinle Group groundwater shows that the alluvial groundwater has the signature of isotope fractionation related to denitrification, a relation of 1:~2 (Bottcher et al. 1990) (Fig. 5). The alluvial groundwater relation is 1:2.3 (Fig. 5) and the Chinle Group wells do not have the 1:2.3 relation suggesting that denitrification does not affect the Chinle Group wells. Denitrification reactions can produce intermediates such as nitrite and nitrous oxide that will abiotically oxidize U(IV) to U(VI), which could be the case in the alluvial aquifer (Nolan and Weber 2015; Senko et al. 2002). In addition, based on data presented in Bottcher et al. (1990), the alluvial and Chinle Group wells with lower δ^{18}O-nitrate and δ^{15}N-nitrate values (P3, ND, and CW37) may be affected by nitrogen fertilizers.

Multivariate statistics

PCA, NMDS, and cluster analysis were used to identify important geochemical fingerprints for further evaluation. Principal component 1 (PC1) accounts for 65.45% of the variance in this dataset and principal component 2 (PC2) accounts for 19.56% of the variance (Fig. 6a, b). Constituents with the highest loadings for PC1, which suggests that these constituents account for the major differences among the geochemistry of the wells, based on the PCA include SO_4^{2-}, Gross beta, ^{228}Ra, U, ^{238}U, ^{234}U, ^{235}U, gross alpha, Mo, Cl, and Na (Fig. 6a). Constituents with the highest loadings for PC2 include Fe, Ca, and Mg, which suggests that these constituents have a secondary effect on the variance in geochemistry among the wells. The distribution of the wells in the plot describes the variability in each well and how each well is associated with other wells (Fig. 6b). For instance, DD, Q, 920, and DD2 plot near each other while CE7 and T11 plot far from all other wells and outside of the 95% prediction ellipse.

The NMDS plot shows a slightly different distribution of the wells compared to the PCA results (Fig. 6c). The clearest differences are the separation of Q from the cluster with 920, DD, and DD2, and the closer distribution of CE7, ST, and T11. The NMDS solution converged after 20 iterations and the stress value was 0.0959442, which is indicative of a robust solution (Buttigieg and Ramette 2014). The cluster analysis shows similar well clusters to the NMDS analysis (Fig. 6d).

When comparing the results from PCA, NMDS, and cluster analysis, the following groups of wells consistently plot together: (1) 920, DD, and DD2; (2) CW15, CW18, ACW, CW28, CW1, CW2; and (3) injectate and ND. The following wells plot near each other in two of the three analyses: (1) CE7, ST, T11; (2) CW45, MV; (3) CW37, P3; and (4) CW50, injectate. Well Q is the only well that does not consistently plot near the other wells, which shows the chemistry is different from nearby wells.

The grouping or clustering is based on statistical comparisons, and certain trends are discernible. The most notable trend is that the local operations at the Site are identifiable at three wells (T11, ST, and CE7) proximal to the site, which relates to U mobility and large U concentrations at these sites (Fig. 4b), and no other wells are associated with this cluster. In contrast, the remaining wells are less distinct from each other and clustered into three groups. Wells proximal to the large tailings pile such as DD and DD2 tend to be associated with regional or local Site impacts.

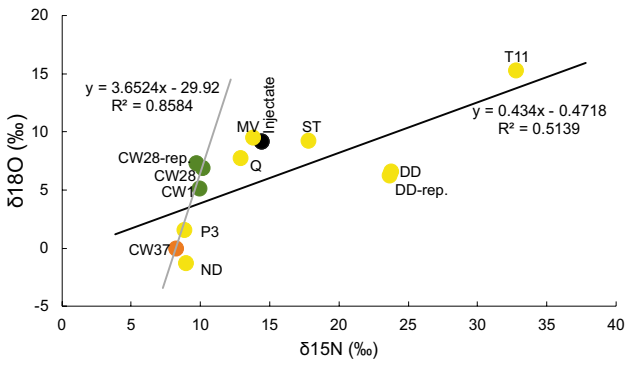

Fig. 5 Plot of δ^{18}O-nitrate vs. δ^{15}N-nitrate. Trendlines are plotted for alluvial aquifer wells (including injectate) and Chinle Group aquifer wells. The alluvial wells have a 1:2.3 relation between δ^{18}O-nitrate and δ^{15}N-nitrate. The Chinle Group aquifer wells do not show the 1:2.3 relation. Yellow circles are alluvial wells, green circles are Middle Chinle Group aquifer wells, orange circles are Upper Chinle Group aquifer wells, and the black circle is the injectate

Radiogenic fingerprints

Uranium isotope ratios

The alluvial well (T11) within the large tailings pile, and the alluvial (ST) and upper Chinle Group well (CE7) directly south of the large tailings pile at the Site, have ^{234}U/^{238}U activity ratios (UAR) of nearly 1 (Fig. 7a). This indicates that the groundwater in these wells has the signature of the mill tailings pile. Groundwater in wells CW45, CW50, MV, Q, P3, and 920 as well as the injectate water have UAR values between 1 and 1.3 (Fig. 7a). There is evidence that UAR values greater than 1.3 are likely unaffected by mining or mill tailings (Zielinski et al. 1997). However, there is also evidence that UAR values may be higher in groundwater in this area because of prolonged interaction with U-rich sediments (Johnson and Wirt 2009; Zielinski et al. 1997). Therefore, based on the UAR values, the wells that have UAR values between 1 and 1.3 may be affected by mining or mill tailings, may have a mix of unaffected and affected

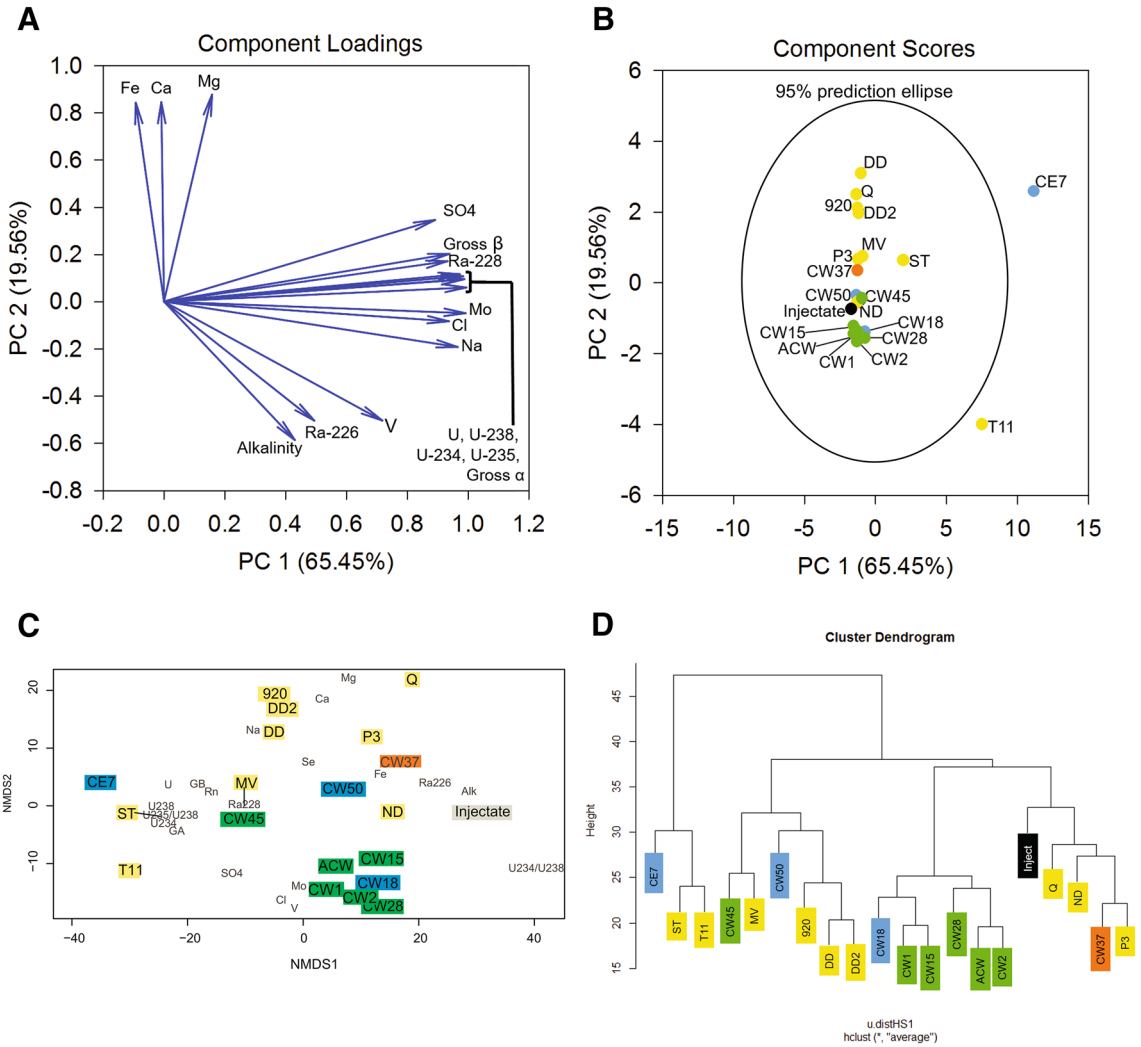

Fig. 6 Plots of multivariate statistical analyses: **a**, **b** PCA, **c** NMDS, and **d** cluster analysis

water, or may be in contact with U-rich sediments for longer periods of time.

Radon

The highest ^{222}Rn activity was found in wells DD2, CE7, T11, and CW50 (Fig. 7b). Wells CE7 and CW50 are screened in the same aquifer, the Upper Chinle Group, where the flow direction is generally from north to south under the tailings pile. Well DD2 is located adjacent to a sub-surface fault (Fig. 1b), where there is potential for ^{222}Rn to seep to the surface. Additionally, well DD2 is near the western evaporation ponds, which could be the source of the radon. T11 is in direct contact with mine tailings, which may explain the elevated ^{222}Rn activity. Radon has a short half-life (3.8 days); therefore, the water sampled from these wells must be near its source for the radon to present in high concentrations. Alternately, the high radon concentrations may be attributed to the high concentrations of parent material (^{226}Ra) in the water.

^{226}Ra and ^{228}Ra

The distribution of ^{226}Ra and ^{228}Ra among the wells shows T11 having the highest concentration of ^{226}Ra (3.82 pCi/L) and CE7 having the highest concentration of ^{228}Ra (5.88 pCi/L) (Fig. 7c). Gallaher and Goad (1981) reported that the San Mateo area discharge from treated mine waters had ^{226}Ra concentrations of 23 ± 1 ($n = 3$) pCi/L and the Ambrosia Lake discharge waters had ^{226}Ra concentrations of 4.6 ± 0.2 ($n = 3$). Both reported ^{226}Ra concentrations are higher than those found in the wells sampled in this study, except for T11. Previous studies in Grants Mineral Belt streams show that ^{226}Ra generally forms insoluble precipitates or adsorbs to sediments within ten river miles of the

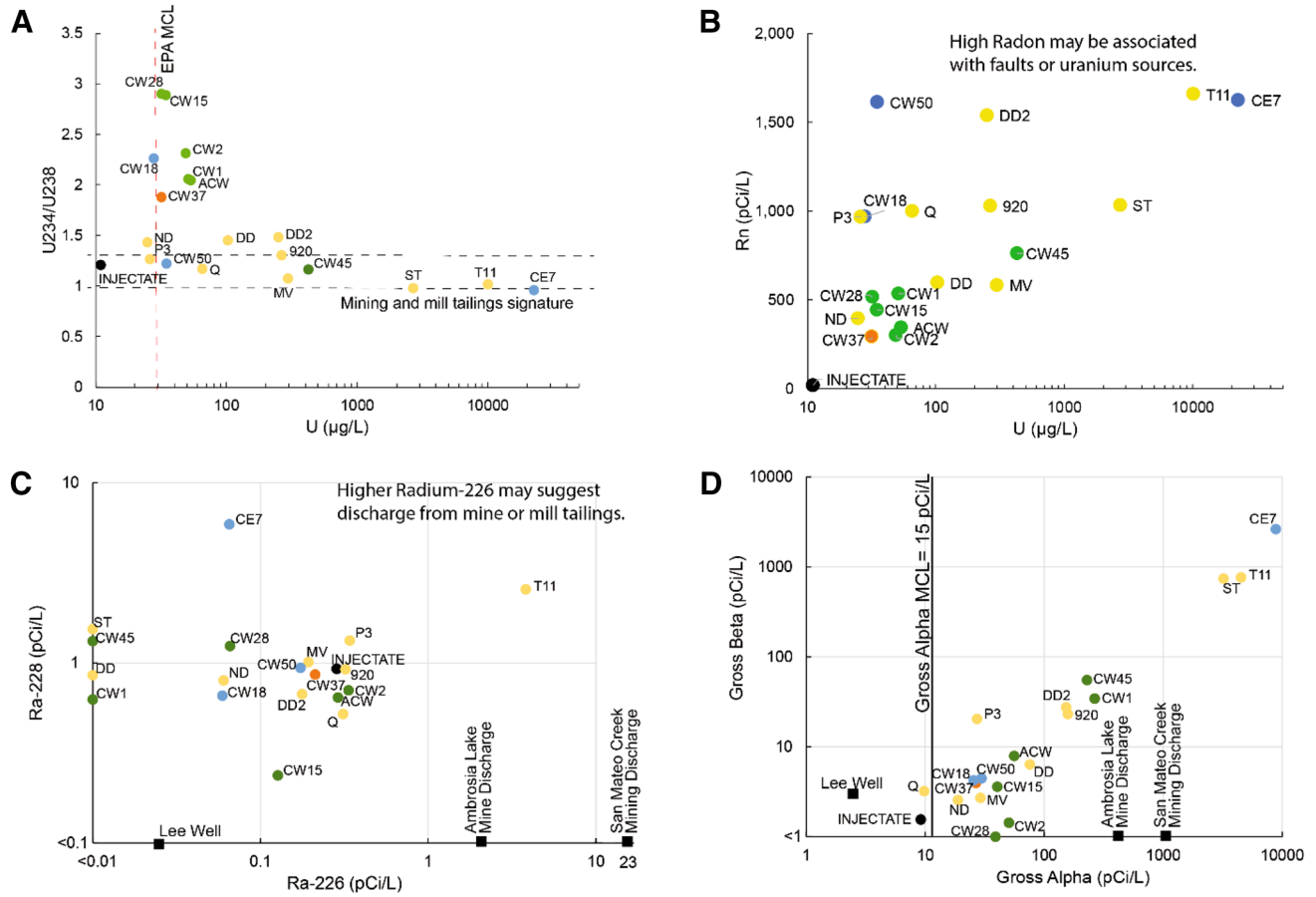

Fig. 7 Plots of **a** $^{234}U/^{238}U$ activity ratio vs. U concentration, **b** Rn concentration vs. U concentration, **c** ^{226}Ra vs. ^{228}Ra (pCi/L), and **d** gross alpha vs. gross beta

source (Gallaher and Cary 1986) and, therefore, ^{226}Ra is not found in high concentrations in groundwater in the area.

Gross alpha–beta

The gross alpha–beta results from the groundwater wells sampled reveal a distribution across the wells (Fig. 7d); eighteen of twenty wells have gross alpha values greater than the 15 pCi/L EPA MCL (EPA 2017), and CE7, ST, and T11 have the highest gross alpha–beta results. The injectate has the lowest gross alpha–beta results (Fig. 7d). Gallaher and Goad (1981) reported that treated mine effluents that discharged to San Mateo Creek and Arroyo del Puerto had gross alpha values of 1100 pCi/L ($n=3$) from the San Mateo Area and 580 ± 70 pCi/L ($n=5$) from the Ambrosia Lake area (Fig. 7d). These values are higher than the gross alpha values reported for the majority of the wells, with the exception of DD2, 920, CW1, CW45, ST, T11, and CE7. These wells with high gross alpha concentrations may have sediments with radioactive materials in contact with the water.

Stable isotopes

The stable isotopes of water (Figure S3) and sulfur (Figure S4) identify general trends of the wells. For instance, the majority of the Chinle Group wells have more negative δD and $\delta^{18}O$ values while the alluvial wells are less negative. The three wells most proximal to the large tailings have high sulfate and less negative $\delta^{34}S$ values. The alluvial wells most north of the large tailings pile have intermediate sulfate concentrations and more negative $\delta^{34}S$ values. Discussion of these trends is included in the SI.

Groundwater travel time

Groundwater travel time between wells Q and MV could be as fast as 0.30 m/day [1 ft/day (365 ft/year)] (Figure S5) as determined by the presence of environmental tracers tritium/helium and CFCs. This suggests that groundwater could travel nearly 10,000 ft (the distance between Q and MV) in 27 years. If mine water discharge in streams recharged the alluvial aquifer a few miles below the confluence of the San

Mateo Creek and Arroyo del Puerto, groundwater from this process would travel to the Site in approximately 60 years.

Source water comparisons in wells

Surface and subsurface structures near the Site reveal a complex interaction of water from mine discharge, Chinle Group and alluvial aquifer mixing and upwelling from faults, effects from the large tailings pile at the Site, and other unidentified sources. Our procedure to interpret the geochemical fingerprinting of groundwater, based on multiple lines of evidence, is shown in Table 1. Our conclusions on sources of water and U in the water are shown in Table 2.

Results suggest that alluvial wells north of the Site have fingerprints from regional sources related to upgradient mining. Alluvial wells on the western side of the Site have regionally upgradient mining water sources, signatures of the mill Site, deeper groundwater or water upwelled from faults, and potentially other sources such as the nearby evaporation ponds. The two alluvial wells closest to the large tailings pile (T11 and ST) and one Upper Chinle Group aquifer well (CE7) directly south of the large tailings pile have the most consistent fingerprints of the local mill tailings. All the deeper Chinle Group wells except two (CW1 and CW2) are mixed with alluvial water that may be affected by the Site water and deeper alluvial groundwater. Deeper groundwater and another unidentified source are the likely source of water in the alluvial well on the eastern side of the Site (ND).

The alluvial wells north of the site, 920, Q, and P3, all appear to have water sourced from regionally upgradient mining based on U concentrations, similar UAR values, and locations within the San Mateo Creek Channel, which may have legacy mining signatures associated with the sediments. Travel time calculated between Wells Q and MV based on age dating suggests that alluvial water may have had time to move the 3000 m (10,000 ft) between the wells (Figure S5; Table S2). Groundwater in wells DD, DD2, and MV not only appears to have regional mining water sources, but also show signatures of the mill Site (DD2 and MV), deeper groundwater or water upwelled from faults (DD2), and potentially other sources (DD2 and DD) such as the nearby evaporation ponds (Fig. 1b). Water in well DD2 may be influenced by the deposition of sediments or infiltration of stream water from the San Mateo Creek channel, but also influenced by the western fault. Wells T11 and ST show the most evidence of water sourced from the mill Site on the basis of U and Mo concentrations, UAR values, and Rn concentrations. Well CE7 also shows evidence of water sourced from the mill Site, but is completed in the Upper Chinle Group aquifer, so it likely has a mixed source of water. Wells ST, T11, and CE7 are directly within or adjacent to the large tailings pile and, therefore, the gross alpha signature may be related to contact with the mill tailings.

Well ND has some geochemical similarities to alluvial wells P3, Q, and the injectate, but may be mixed with deeper aquifer water based on the Piper diagram and passive sampling results reported in Harte et al. (2019). In addition, well ND is located east of the eastern fault and within the Lobo Canyon deposits; therefore, well ND may have another source of water that is unidentified. The injectate water is known to be a mixture of reverse osmosis water and the San Andres-Glorieta Formation aquifer water.

Well CW45 is in the subcrop area at the southern edge of the Site and may be affected by alluvial waters or from upwelling from the eastern fault. Based on knowledge of the subcropped geology in the southern and western portions of the Site, it is suggested that wells CW18, CW15, CW45, ACW and CW28 are within the mixing zone between the alluvial aquifer and the Chinle Group aquifer. In addition, the wells located in the mixing zone and between the two faults, and south of the large tailings pile (ACW, CW15 and CW45) are considered affected by tailings seepage (Hydro-Engineering 2001). All of the Middle Chinle Group wells plot in the End Member 2 area of the Piper Diagram except for sampled well water from CW45, which plots in the mixed area. In addition, CW45 plots closer to MV in the NMDS biplot and the cluster analysis, which may provide further evidence of mixed water.

Well CW50 is north of the large tailings pile and in the upper Chinle Group aquifer. This well may be a mixture of

Table 2 Wells sampled in this study with their likely source(s) of water

Water source	920	Q	ND	DD2	DD	P3	T11	ST	MV	CW50	CE7	CW18	CW1	CW2	ACW	CW15	CW45	CW28	CW37	INJECTATE
1. Regionally sourced from upgradient mining	X	X		X	X	X			X											
1a. San Mateo Creek Channel	X	X		X		X														
2. Locally sourced by the mill Site				X			X	X	X	X	X	X			X	X	X	X	X	
3. Sourced from deeper aquifer groundwater			X	X						X	X	X	X	X	X	X	X	X	X	
3a. Near fault			X	X													X			
3b. Near Subcrop												X			X	X	X	X		
4. Other source			X	X	X															X

The alluvial aquifer wells are highlighted in yellow, Upper Chinle Group aquifer in blue, Middle Chinle Group aquifer in green, and Lower Chinle Group aquifer in orange. The injectate water is shown in black. Samples within each aquifer are listed from north to south

alluvial and Chinle Group water, as supported by the Piper Diagram, multivariate analysis, and UAR. Additionally, well CW50 had the highest Rn concentration of all wells, which may indicate radioactive sediments. This well is not close to either fault. Well CW37 is the only lower Chinle Group well sampled and may have a mixture of alluvial and Chinle Group water, as shown in the Piper diagram and multivariate analysis. Wells CW1 and CW2 are slightly north of the large tailings pile and are in the Middle Chinle Group aquifer. Both wells plot in End Member 2 on the Piper Diagram but have UAR values above 1.3 and low Rn concentrations, which may indicate that the water is predominantly from the Chinle Group aquifer. The Chinle Group waters with an X in the 'locally sourced by the mill Site' category in Table 2 may contain waters affected by the Site, but further study is required to identify this source.

Conclusions

The Homestake uranium mill site is a very complex hydrogeological system because of the geology, naturally occurring elements, and various anthropogenic effects at the Site and north of the Site. To understand the sources of U in each sampled groundwater well, a geochemical fingerprinting approach was used to define water sources to aid in understanding the source of U to the wells. Multiple lines of evidence, including general chemistry, stable isotopes, radiogenic isotopes, borehole geophysics, groundwater age dating, and multivariate statistics were used to differentiate sources of U and other associated compounds. This research has shown that combining geochemical fingerprinting, multivariate statistics, subsurface structure, and spectral gamma coupled with passive sampling (Harte et al. 2019) is an effective approach to understand the source of water and U in groundwater to wells nearby the Site. The multivariate statistics provided quantitative analyses of the data, which clustered wells into groups based on groundwater chemistry. The commonalities among the statistical approaches provide robust support for similarities among groundwater samples from sets of wells obtained by geochemical fingerprints.

In general, the wells proximal to the large tailings pile have the highest U concentration, Rn activity, gross alpha and beta, and UAR closest to 1. Most of the wells studied have U concentrations higher than the MCL of 30 µg/L and appear to be affected by regional sources of U. However, the injectate water, which has been treated and mixed with San Andres-Glorieta Formation aquifer groundwater, has the lowest U concentration. Geochemistry of the alluvial wells north of the Site may be influenced by San Mateo Creek channel sediments, although further analysis is needed to understand the mechanisms associated with this finding. Wells south of the Site have mixed groundwater sources, likely because of the complexity of the hydrogeology and flow paths of groundwater in the aquifers.

The approach used in this study provides results that can be used by land managers and regulators to determine which wells best represent background concentrations for sites that have multiple effects from naturally occurring contaminants and anthropogenic contaminants. However, the data collected in this study are from one point in time. Seasonal geochemical variability was not assessed. Samples from wells reflect a mixture of water sources, partly from the installation of well screens or well openings (in open boreholes) that cross multiple types of units and formations (Harte et al. 2019). Installation of short-screen monitoring wells would help reduce mixing with the goal of collecting samples more representative of specific groundwater flow paths. Further research could include analyzing the chemistry of subsurface sediments, which could further define the geochemical interactions between these sediments and groundwater. In addition, sampling of more wells in the area, including those north of the Site, could provide information about the chemistry of the groundwater throughout the area. The results provide a new method to fingerprint groundwater and differentiate among water sources, which will aid regulators in decisions about background concentrations of U in groundwater near the Site and provide scientists with an additional geochemical fingerprinting approach.

Acknowledgements The authors would like to thank the EPA remedial project manager Sai Appaji for his support on this study. We thank the employees at Homestake Mill who helped locate wells, pulled pumps to allow for sampling, explained safety protocols for the site, helped field crews (stuck in mud), and for their courtesy to our staff while working on-site. We thank the local community for their interest in this site. In addition, a big thanks goes the following USGS staff who helped collect the data: Jon Thomas, Dominick Antolino, Chris Braun, Becky Lambert, and Doug Nagle. We also thank Katie Walton-Day, Kim Beisner, and Ryan McCutcheon for their reviews of this manuscript. Landowners adjacent to the site supported our work before and during the data collection process. Any use of trade, firm, or product names is for descriptive purposes only and does not imply endorsement by the U.S. Government.

References

Abdelouas A (2006) Uranium mill tailings: geochemistry, mineralogy, and environmental impact. Element 2:335–341

Agency for Toxic Substances and Disease Registry (ATSDR) (2009) Health Consultation, Homestake Mining Company Mill Site, Milan, Cibola County, New Mexico. https://www.atsdr.cdc.gov/hac/pha/homestake/homestakemcojun091.pdf Accessed 31 Oct 2017

Alam MS, Cheng T (2014) Uranium release from sediment to groundwater: influence of water chemistry and insights into release mechanisms. J Contam Hydrol 164:72–87. https://doi.org/10.1016/j.jconhyd.2014.06.001

Baldwin JA, Anderholm SK (1992) Hydrogeology and ground-water chemistry of the San Andres-Glorieta aquifer in the Acoma

Embayment and Eastern Zuni Uplift, West-Central, New Mexico. U.S. Geological Survey Water Resources Investigations Report, 91-4033

Baldwin JA, Rankin DR (1995) Hydrogeology of Cibola County, New Mexico. U.S. Geological Survey Water-Resources Investigations Report, 94-4178

Basu A, Brown ST, Christensen JN, DePaolo DJ, Reimus PW, Heikoop JM, Woldegabriel G, Simmons AM, House BM, Hartmann M, Maher K (2015) Isotopic and geochemical tracers for U(VI) reduction and U mobility at an in situ recovery U mine. Environ Sci Technol 49(10):5939–5947. https://doi.org/10.1021/acs.est.5b00701

Blake JM, DeVore CL, Avasarala S, Ali A, Roldan C, Bowers F, Spilde MN, Artyushkova K, Kirk MF, Peterson E, Rodriguez-Freire L, Cerrato JM (2017a) Uranium mobility and accumulation along the Rio Paguate, Jackpile Mine in Laguna Pueblo, NM. Environ Sci Process Impact 19:605. https://doi.org/10.1039/c6em00612d

Blake JMT, Becher KD, Harte PT, Thomas JV, Stengel VG (2017b) Data associated with uranium background concentrations at Homestake Mining Company Superfund Site, near Milan, New Mexico, July 2016 through October 2016 (ver. 1.1, August 2017). U.S. Geological Survey data release, https://doi.org/10.5066/F7CR5RJS

Borch T, Kretzschmar R, Kappler A, Van Cappellen P, Ginder-Vogel M, Vogelin A, Campbell K (2010) Biogeochemical redox processes and their impact on contaminant dynamics. Environ Sci Technol 44:15–23. https://doi.org/10.1021/es9026248

Bottcher J, Strebel O, Voerkelius S, Schmidt HL (1990) Using isotope fractionation of nitrate-nitrogen and nitrate-oxygen for evaluation of microbial denitrification in a sandy aquifer. J Hydrol 114:413–424

Briganti A, Armiento G, Nardi E, Proposito M, Tuccimei P (2017) Understanding uranium behaviour in a natural rock–water system: leaching and adsorption tests on the Tufo Rosso a Scorie Nere ignimbrite (Viterbo area, central Italy). Environ Earth Sci 76:680. https://doi.org/10.1007/s12665-017-7010-1

Brod RC and Stone WJ (1981) Hydrogeology of Ambrosia Lake-San Mateo area, McKinley and Cibola Counties, New Mexico. New Mexico Bureau of Mines and Mineral Resources Hydrogeologic Sheet 2

Brookins DG (1977) Uranium deposits of the Grants Mineral Belt: geochemical constraints on origin. Exploration Frontiers of the Central and Southern Rockies, pp 337–352

Buttigieg PL, Ramette A (2014) A guide to statistical analysis in microbial ecology—a community-focused, living review of multivariate data analyses. FEMS Microbiol Ecol 90:543–550

Cather S (2011) Geologic map of the Dos Lomas quadrangle, Cibola and McKinley Counties, New Mexico. New Mexico Bureau of Geology and Mineral Resources, Open-File Geologic Map 219. https://geoinfo.nmt.edu/publications/maps/geologic/ofgm/downloads/219/DosLomas.pdf. Accessed 21 Feb 2018

Christensen JN, Dressel PE, Conrad M, Maher K, Depaolo DJ (2004) Identifying the sources of subsurface contamination at the Hanford Site in Washington using high precision Uranium isotopic measurements. Environ Sci Technol 38(12):3330–3337

Corcho J, Balsiger B, Rollin S, Burger M (2015) 234U/238U isotopic ratio in water as indicator of uranium contamination: a study case in Mailuu-Suu (Kyrgyzstan), Conference presentation: International Symposium on Isotope Hydrology: Revisiting Foundations and Exploring Frontiers At: IAEA, Vienna. https://www.researchgate.net/publication/279921097_234U238U_isotopic_ratio_in_water_as_indicator_of_uranium_contamination_A_study_case_in_Mailuu_Suu_Kyrgyzstan. Accessed 22 May 2019

de Carvalho Filho CA, Moreira RM, Branco OEA, Dutra PH, Dos Santos EA, Moura IFS, Fleming PM, Palmieri HEL (2017) Combined hydrochemical, isotopic, and multivariate statistics techniques to assess the effects of discharges from a uranium mine on water quality in neighboring streams. Environ Earth Sci 76:830. https://doi.org/10.1007/s12665-017-7165-9

Dong W, Brooks SC (2006) Determination of the formation constants of ternary complexes of uranyl and carbonate with alkaline earth metals (Mg^{2+}, Ca^{2+}, Sr^{2+}, and Ba^{2+}) using anion exchange method. Environ Sci Technol 40:4689–4695. https://doi.org/10.1021/es0606327

Fetter CW (2001) Applied hydrogeology. Prentice Hall, New Jersey, p 598

Gallaher BM, Cary SJ (1986) Impacts of uranium mining on surface and shallow ground waters: Grants Mineral Belt, New Mexico. New Mexico Environmental Improvement Division, EID/GWH-86/2

Gallaher BM, Goad MS (1981) Water-quality aspects of uranium mining and milling in New Mexico. In: Wells SG, Lambert W, Callender JF (eds) Environmental geology and hydrology in New Mexico. New Mexico Geological Society Special Publication 10, Socorro, pp 85–91. http://geoinfo.nmt.edu/publications/nmgs/special/10/. Accessed 10 May 2018

Hall SM, Mihalasky MJ, Tureck KR, Hammarstrom JM, Hannon MT (2017) Genetic and grade and tonnage models for sandstone-hosted roll-type uranium deposits, Texas Coastal Plain, USA. Ore Geol Rev 80:716–753. https://doi.org/10.1016/j.oregeorev.2016.06.013

Harte PT, Blake JM, and Becher KD (2018a) Determination of representative uranium and selenium concentrations from groundwater, 2016, Homestake Mining Company Superfund site, Milan, New Mexico: U.S. Geological Survey Open-File Report 2018–1055, appendixes. https://doi.org/10.3133/ofr20181055

Harte PT, Blake JMT, Becher KD, Thomas JV, Stengel VG (2018b) Data associated with uranium background concentrations at Homestake Mining Company Superfund site, near Milan, New Mexico, July 2016 through October 2016 (ver. 1.2, September 2018). U.S. Geological Survey Data Release. https://doi.org/10.5066/F7CR5RJS. Accessed 9 Oct 2018

Harte PT, Blake JM, Thomas J, Becher K (2019) Identifying natural and anthropogenic variability of uranium at the well scale, Homestake Superfund site, near Milan, New Mexico, USA. Environ Earth Sci 78:95. https://doi.org/10.1007/s12665-019-8049-y

Homestake Mining Company and Hydro-Engineering, LLC (2004) Grants reclamation project background water quality evaluation of the Chinle Aquifers. https://www.nrc.gov/docs/ML0331/ML033160203.pdf. Accessed 10 May 2018

Homestake Mining Company and Hydro-Engineering, LLC (2014) 2013 Annual monitoring report/performance review for Homestake's Grants project pursuant to NRC license SUA-1471 and Discharge plan DP-200. https://www.nrc.gov/docs/ML1409/ML14093A305.pdf. Accessed 10 May 2018

Homestake Mining Company of California (2012) Grants reclamation project updated corrective action program (CAP). https://www.nrc.gov/docs/ML1208/ML12089A057.pdf. Accessed 10 May 2018

Hydro-Engineering, LLC (2001) Ground-water hydrology for support of background concentration at the Grants Reclamation Site for Homestake Mining Company of California. https://www.nrc.gov/docs/ML0331/ML033140215.pdf. Accessed 10 May 2018

Ingraham NL (1998) Isotopic variations in precipitation. In: Kendall C, McDonnell JJ (eds) Isotope tracers in catchment hydrology. Elsevier Science B.V, Amsterdam, pp 87–118

Jensen ML (1963) Sulfur isotopes and biogenic origin of uraniferous deposits of the Grants and Laguna Districts, Geology and Technology of the Grants Uranium Region, Memoir 15. State Bureau of Mines and Mineral Resources, Socorro, pp 182–190

Jiang Y, Guo H, Jia Y, Cao Y, Hu C (2015) Principal component analysis and hierarchical cluster analyses of arsenic groundwater geochemistry in the Hetao basin, Inner Mongolia. Chem Erde 75:197–205

Johnson RH, Wirt L (2009) Geochemical analyses of rock, sediment, and water from the region in and around the Tuba City Landfill, Tuba City, Arizona. U.S. Geological Survey Open-File Report 2009–1020

Johnson RH, Gover BPC, Tutu H (2016) Prediction of uranium transport in an aquifer at a proposed uranium in situ recovery site: Geochemical modeling as a decision-making tool. In: Saleh HEM, Rahman, ROA (eds) Management of hazardous wastes. https://doi.org/10.5772/63537

Kamp SD, Morrison SJ (2014) Use of chemical and isotopic signatures to distinguish between uranium mill-related and naturally occurring groundwater constituents. Ground Water Monit Remediat 34(1):68–78. https://doi.org/10.1111/gwmr.12042

Kaufman RF, Eadie GG, Russel CR (1976) Effects of uranium mining and milling on groundwater in the Grants Mineral Belt, New Mexico. Ground Water 14(5):296–308

Kendall C, Caldwell EA (1998) Fundamentals of isotope geochemistry, Chapter 2. In: Kendall CC, McDonnell JJ (eds) Isotope tracers in catchment hydrology. Elsevier Science B.V, Amsterdam, pp 51–86

Langman JB, Sprague JE, Durall RA (2012) Geologic framework, regional aquifer properties (1940s–2009), and spring, creek and seep properties (2009–10) of the Upper San Mateo Creek Basin near Mount Taylor, New Mexico. U.S. Geological Survey Scientific Investigations Report 2012-5019

Leavitt JJ, Howe KJ, Cabaniss SE (2011) Equilibrium modeling of U(VI) speciation in high carbonate groundwaters: model error and propagation of uncertainty. Appl Geochem 26:2019–2026. https://doi.org/10.1016/j.apgeochem.2011.06.031

Morrison SJ, Spangler RR (1992) Extraction of uranium and molybdenum from aqueous solutions: a survey of industrial materials for use in chemical barriers for uranium mill tailings remediation. Environ Sci Technol 26:1922–1931

New Mexico Bureau of Geology and Mineral Resources (NMBGMR) (2003) Geologic map of New Mexico, scale 1:500,000. https://geoinfo.nmt.edu/publications/maps/geologic/state/home.cfml. Accessed 2017

New Mexico Environment Department (NMED) (2008) Preliminary assessment report: San Mateo Creek legacy uranium sites. https://www.epa.gov/sites/production/files/2015-06/documents/06-93397 67.pdf. Accessed 10 May 2018

New Mexico Environment Department (NMED) (2012) Site inspection report, Phase 2, San Mateo Creek Basin legacy uranium mine and mill site area, CERCLIS ID NMN000606847, Cibola-McKinley Counties, New Mexico. https://www.epa.gov/sites/production/files/2015-05/documents/san_mateo_creek_si_phase_2-report_final.pdf. Accessed 10 May 2018

Nolan J, Weber KA (2015) Natural uranium contamination in major U.S. aquifers linked to nitrate. Environ Sci Technol Lett 2:215–220. https://doi.org/10.1021/acs.estlett.5b00174

Nuclear Regulatory Commission (1981) Appendix A—report on alkaline carbonate leaching at Homestake Mining Company, https://www.nrc.gov/docs/ML0702/ML070240368.pdf. Accessed 16 June 2018

Parkhurst DL, Appelo CAJ (1999) User's guide to PHREEQC (Version 2)—A computer program for speciation, batch-reaction, one-dimensional transport, and inverse geochemical calculations. U.S. Geological Survey Water-Resources Investigations Report 99-4259

Popp CJ, Hawley JW, Love DW (1983) Radionuclide and heavy metal distribution in recent sediments of major streams in the Grants Mineral Belt, N.M. Washington, D.C., U.S. Department of Interior, Final Report to Office of Surface Mining

Ries KS (1982) Stable oxygen and sulfur isotopes applied to tracing seepage from mine tailings. Master's Thesis, The University of Arizona. http://hdl.handle.net/10150/191770. Accessed 12 Feb 2018

Robertson AJ, Ranalli AJ, Austin SA, Lawlis BR (2016) The source of groundwater and solutes to Many Devils Wash at a former uranium mill site in Shiprock, New Mexico. U.S. Geological Survey Scientific Investigations Report 2016–5031. https://doi.org/10.3133/sir20165031

Roca Honda Resources, LLC (2011) Baseline Data Report, Section 8.0, Surface Water. http://www.emnrd.state.nm.us/MMD/MARP/permits/documents/MK025RN_201101_Roca_Honda_Baseline_Report_Rev1_Section8_Surface_Water.pdf. Accessed 6 Nov 6 2017

Sahu P, Panigrahi DC, Mishra DVP (2016) A comprehensive review on sources of radon and factors affecting radon concentration in underground uranium mines. Environ Earth Sci 75:617. https://doi.org/10.1007/s12665-016-5433-8

Schoeppner J (2008) Groundwater remediation from uranium mining in New Mexico. Southwest Hydrol. November/December issue:22–23

Senko JM, Istok JD, Suflita JM, Krumholz LR (2002) In-situ evidence for uranium immobilization and remobilization. Environ Sci Technol 36:1491–1496. https://doi.org/10.1021/es011240x

Turner-Peterson CE, Fishman ES (1986) Fluvial sedimentology of a major uranium-bearing sandstone—a study of the Westwater Canyon Member of the Morrison Formation, San Juan basin, New Mexico. In: Turner-Peterson CE, Santos ES, Fishman NS (eds) A basin analysis case study: The Morrison Formation, Grants Uranium Region, New Mexico, vol 22. American Association of Petroleum Geologists Studies in Geology, pp 47–75

U.S. Environmental Protection Agency (EPA) (2008) Technical Report on Technologically Enhanced Naturally Occurring Radioactive Materials from Uranium Mining Vol. 1: Mining and Reclamation Background. U.S. Environmental Protection Agency, Office of Radiation and Indoor Air, EPA 402-R-08-005: Washington, D.C.

U.S. Environmental Protection Agency (EPA) (2011) Third Five-Year Review Report, Homestake Mining Company Superfund Site, Cibola County, New Mexico. U.S. Environmental Protection Agency, Region 6, Dallas

U.S. Environmental Protection Agency (EPA) (2017) Drinking water requirements for states and public water systems. Radionuclides rule. https://www.epa.gov/dwreginfo/radionuclides-rule#rule-summary. Accessed 22 Feb 2018

U.S. Geological Survey (USGS) (2004) National Uranium Resource Evaluation (NURE) Hydrogeochemical and Stream Sediment Reconnaissance data: U.S. Geological Survey, Denver. https://mrdata.usgs.gov/nure/sediment/ and https://mrdata.usgs.gov/nure/water/. Accessed 13 Nov 2017

U.S. Geological Survey (USGS) (2006) Collection for water samples (ver. 2.0). U.S. Geological Survey Techniques for Water-Resources Investigations, book 9, chap. A4, September 2006. http://pubs.water.usgs.gov/twri9A4/. Accessed 10 May 2018

U.S. Geological Survey (USGS) (2015) Program for creating specialized graphs used in groundwater studies, version 1.29. https://water.usgs.gov/nrp/gwsoftware/GW_Chart/GW_Chart.html. Accessed 10 May 2018

U.S. Geological Survey (USGS) (2018) USGS water data for the Nation. U.S. Geological Survey National Water Information System database. https://doi.org/10.5066/F7P55KJN. Accessed 1 Apr 2018

Van Berk W, Fu Y (2017) Redox roll-front mobilization of geogenic uranium by nitrate input in aquifers: risks for

groundwater resources. Environ Sci Technol 51:337–345. https://doi.org/10.1021/acs.est.6b01569

Van Metre PC, Wirt L, Lopes TJ, Ferguson SA (1997) Effects of uranium-mining releases on ground-water quality in the Puerco River Basin, Arizona and New Mexico. U.S. Geological Survey Water-Supply Paper 2476

Vengosh A (2003) Salinization and saline environments. In: Holland HD, Turekian KK, Sherwood Lollar B (eds) Treatise on geochemistry, vol 9. Elsevier Sciences, Amsterdam, pp 333–365

Weston Solutions, Inc. (2016) Expanded site inspection Phase 1-Groundwater investigation report for San Mateo Creek Basin uranium legacy site: Cibola and Mckinley Counties, New Mexico. https://www.epa.gov/sites/production/files/2016-11/documents/epa_smcb_esi_phase1.pdf. Accessed 17 June 2018

Yabusaki SB, Fang Y, Long PE, Resch CT, Peacock AD, Komlos J, Jaffe PR, Morrison SJ, Dayvault RD, White DC, Anderson RT (2007) Uranium removal from groundwater via in situ biostimulation: field-scale modeling of transport and biological processes. J Contam Hydrol 93:216–235

Zielinski RA, Chafin DT, Banta ER, Szabo BJ (1997) Use of ^{234}U and ^{238}U isotopes to evaluate contamination of near-surface groundwater with uranium-mill effluent: a case study in south-central Colorado, U.S.A. Environ Geol 32(2):124–136

Differentiating anthropogenic sources of uranium by geochemical fingerprinting of groundwater at the Homestake Uranium Mill, New Mexico, USA.

Supplemental Information

Johanna M. Blake[1*], Phil Harte[2], Kent Becher[3]

*Corresponding author email- jmtblake@usgs.gov
Telephone- 505-830-7953.

[1]U.S. Geological Survey, 6700 Edith Blvd. NE, Albuquerque, NM 87113,
https://orcid.org/0000-0003-4667-0096
[2]U.S. Geological Survey, 720 Gracern Rd., Columbia, SC 29210
https://orcid.org/0000-0002-7718-1204
[3]U.S. Geological Survey, 501 W. Felix Street Bldg 24, Fort Worth, TX 76133
https://orcid.org/0000-0002-3947-0793

Sample collection, methods, and preservation

Prior to volumetric purging, the depth of the well was sounded and the water level measured from an established measurement point. For monitoring wells, three casing volumes were purged and field parameters monitored for field stabilization. For the monitoring wells without existing pumps, a variable speed submersible pump was used. For existing remedial extraction wells, residential wells in use, and select monitoring wells, the existing pumping infrastructure was used. For residential wells offline but with existing pump equipment, the well was pumped for three volumes similar to monitoring wells. During purging for all wells, physiochemical water-quality characteristics were recorded including water temperature, specific conductivity, pH, dissolved oxygen, and turbidity. Collection and preservation techniques are described in Table S1.

Constituents for chemical analyses selected to facilitate identification of water type include: alkalinity, major anions (total and dissolved), major cations (total and dissolved), selected trace elements (total and dissolved), total dissolved solids, nitrate (dissolved), gross alpha/beta, radium isotopes, radon-222, uranium isotopes and stable isotopes of deuterium (δD) and oxygen-18 (δ18O), sulfur isotopes of sulfur and oxygen isotopes of sulfate, nitrogen isotopes of nitrogen and oxygen isotopes of nitrate, carbon-14, dissolved gases, tritium/helium-3, chlorofluorocarbons (CFCs), and helium-4. Analyses were completed at RTI Laboratories, EPA Region 6 Laboratory, PACE Laboratories, USGS Reston Stable Isotope Laboratory, USGS Reston Groundwater Dating Laboratory, Woods Hole, and University of Utah. Analytical methods are documented in Table S1. Data were evaluated from each lab for quality control (Blake et al. 2017b). For some wells, U concentrations from RTI Laboratories were adjusted as determined by the EPA Region 6 Laboratory after methods described by Harte et al. (2018).

Multivariate technique methods

Principal component analysis (PCA) represents a transformed axis that is a linear combination of the original variables (Kimball et al. 2004) and simplifies the information into the most important factors that account for data variance. PCA can be used to systematically evaluate the geochemistry of groundwater from the wells in question and distinguishes similarities and differences among the wells. The first two principal components (PC1 and PC2) generally show enough variance in the data to differentiate groups among the samples (Kimball et al. 2004). Each chemical constituent has an associated component loading that shows the correlation between the constituent and the PCA (Kimball et al. 2004). The component loadings measure the degree to which the identified components account for the geochemical composition of the data in each well. The PCA was calculated using SigmaPlot V13.0 (SigmaPlot 2018). Within SigmaPlot, the raw data are normalized based upon a correlation matrix where each variable is standardized to have unit sample variance. The PCA is calculated using the normalized data. The PCA produces a biplot of PC1 versus PC2 and the location of the wells within this space. A 95% prediction ellipse is calculated and plotted on the biplot to show possible outliers in the distribution of data (SigmaPlot 2018).

Data variance was further evaluated by using non-metric multidimensional scaling (NMDS) and cluster analysis routines in the R packages NADA and VEGAN (Lee 2015; Oksanen and others 2016). NMDS is a non-parametric approach to PCA, that uses rank order rather than data values (Buttigieg and Ramette 2014) and produces an ordination based on distance matrix. Both PCA and NMDS produce biplots of the location of wells where samples that plot closer to each other are more similar. Cluster analysis hierarchically clusters data to

minimize the sum of squares of any two clusters (Jiang et al. 2015) and can be evaluated similarly to PCA or NMDS as the results help to distinguish similarities and differences among samples.

Table S1: Constituents, method, containers, preservatives, and holding times for analytical methods. Dissolved constituents were filtered with a 0.45-µm filter.

[ml, milliliter; oz, ounce; C, Celsius; CFC, chlorofluorocarbon; ml, milliliter; HNO3, Nitric acid; µm, micrometer]

Description	Method	Container	Preservation	Holding Time
Metals	6020	250-ml plastic	HNO_3 , 4° C	180 days
Alkalinity	SM2320B	250-ml plastic	4° C	14 days
Ammonia	SM4500	250-ml plastic	H_2SO_4 , 4° C	28 days
Br, CL, F, SO_4	300	120-ml plastic	4° C	28 days
Nitrogen	SM4500	250-ml plastic	H_2SO_4 , 4° C	28 days
Gross alpha/beta	900	250-ml plastic	pH<2 HNO_3	180 days
Radium isotopes	903.1/904	250-ml plastic	pH<2 HNO_3	180 days
Uranium isotopes	HASL 300	250-ml plastic	pH<2 HNO_3	180 days
Carbon-14	Liquid scintillation	500-ml polyethylene bottle	none	180 days
Radon-222	Liquid scintillation	3-40 ml vials		3 days
Stable isotopes of deuterium (δD) and oxygen-18 (δ18O)	Révész and Coplen (2008)	2-oz (60 ml) glass with polyseal cap	Store at ambient temperature	Months
Sulfur isotopes	Révész et al. (2012)	1-Liter polyethylene bottle	Filtered with 0.4-µm polycarbonate membrane filter	Months
Nitrogen isotopes	Coplen et al. (2012)	4-oz (125 ml) amber polyethylene bottle	Filtered with 0.4-µm polycarbonate membrane filter followed by a 0.2-µm syringe filter, freeze sample	Months
He-4	Révész and Coplen (2000A and B)	3 septum glass bottles (150 ml)	4° C	3 years
Dissolved gases		copper tubing, properly sealed	none	years
Tritium/He-3		2-500 cc (16 oz) Nalgene plastic bottle)	none	years

CFCs		5-125 ml Boston round clear glass bottles with cap with an aluminum foil linear	none	30 days

Stable Isotopes of Water (δD and $\delta^{18}O$)

The δD and $\delta^{18}O$ values in the groundwater samples generally plot between the Local Meteoric Water Line (LMWL) and the Arid Meteoric Line (AML) (Figure S3). Samples T11, ND, CE7, CW37, and the Injectate plot along a reduced slope below the AML, which is indicative of fractionation due to evaporation (Langman et al. 2012). Well ND had the heaviest isotopic signature for δD and $\delta^{18}O$ δD and $\delta^{18}O$ values, which may indicate different source water than in other alluvial wells. In general, the middle Chinle Group wells have lighter stable isotope values, which suggests either colder temperatures during recharge or differences in source waters compared to most of the alluvial well samples (Langman et al. 2012). Well water plotting with heavier per mil (less negative) are likely experiencing some shallow recharge and affected more so by evaporation, whereas well water intercepting deeper recharge is lighter (more negative) per mil. It is likely that recharge temperatures were appreciably colder for the deeper wells suggesting mixing of some older waters. The main difference is likely the amount of shallow recharge mixing in with the wells on the bottom having the least shallow recharge. Well DD2, which is located adjacent to the western fault, has heavier stable isotope values compared to well DD, and has similar stable isotope values compared to well P3, which is located between the two faults. This pattern may indicate that the recharge to well DD2 is from both surface recharge and upwelling from deeper groundwater through the fault. The combination of this result and the radon results in figure 7b showing DD2 with 1,500 pCi/L Rn

and P3 showing 950 pCi/L Rn may suggest that groundwater at DD2 is a mixture of surface recharge water (potentially affected by the proximity to the western evaporation pond) and upwelling of water from the western fault. Well DD2 was positioned within a low-lying surface depression that may be susceptible to focused recharge and stream runoff.

Stable Isotopes of Sulfur (δ34S)

There is not a clear signature of mining, milling, or background based on the δ34S data. Nine (CW45, CW28, CW2, CW1, ACW, CW37, Injectate, MV, and ST) of the nineteen groundwater wells analyzed for δ34S had values ranging from -5‰ to 5‰, which is the δ34S range identified from water in tailings ponds and groundwater near uranium mill sites in the Grants Mineral Belt and Navajo Nation (Kamp and Morrison 2014) (Figure S4). The middle and lower Chinle Group wells that plot within -5‰ to 5‰ do not show corresponding mill fingerprints as seen with the UAR, which may indicate that the Chinle Group groundwater is mixed with alluvial water or that the δ34S signatures of these wells are indicative of sulfur in the surrounding geology (Ries, 1982; Karim and Veizer 2000). Groundwater from wells Q, DD2, DD, P3, CW50, and CW15 have more negative δ34S values than from other wells, that may indicate mine discharge or contact with sulfides in the alluvium and Chinle Group (Figure S4). Data from the Arroyo del Puerto mine discharge and Ambrosia Lake mill site show a range of $\delta^{34}S$ from -28.4‰ to +10.4‰ (Ries 1982), which encompasses nearly all of the δ34S results for the wells. Sedimentary sulfides, typically the mineral pyrite, have a $\delta^{34}S$ range -50‰ to 10‰ but most values are negative (Karim and Veizer 2000); pyrite in sandstone-type uranium deposits in the Grants Mineral Belt has a $\delta^{34}S$ range of -27‰ to -1.8‰ (Jensen 1963). However, the differences in δ34S between ST, T11, CE7 and P3, CW50, DD2, DD, Q is approximately 20 per mil, which may indicate different sources of SO_4. For instance, the Ambrosia Lake mill site

used sulfuric acid during mill processes (Ries 1982) and the Homestake mill site used alkaline leaching (Nuclear Regulatory Commission 1981). The oxidation of pyrite contained in mill tailings may result in the release of sulfuric acid, which could also be a signature of mill sites (Landa 1980).

Well T11 and CE7 have the highest SO_4 concentrations, which can be associated with the proximity to the uranium tailings piles (Ries 1982). In addition, there is clear cutoff between the dissolution of sulfate minerals compared to the oxidation of sulfate minerals around -8‰, which may be a control on U mobility. Availability of pyrite and sulfur oxidation can impact U mobilization by oxidation of U(IV) to U(VI) thereby mobilizing U(VI) (Basu et al. 2015).

Age Dating

Chemical and isotopic constituents that have been released into the atmosphere at unique rates and interact with atmospheric water may be introduced to the groundwater and can be used to estimate the apparent age of groundwater (Plummer and Friedman, 1999). Tritium (^3H) is a short-lived radioactive isotope of hydrogen, with a half-life of 12.32 years (Lucas and Unterweger 2000). These ^3H concentrations from nuclear weapons testing continue to be present in some groundwater and may be used to qualitatively constrain the recharge date (Clark and Fritz, 1997). These methods are good for dating groundwater with an age of less than 100 years. The refrigerant CFC-12 was the first chlorofluorocarbon produced, and its presence in groundwater indicates that recharge occurred after 1940. The presence of CFC-11 indicates that recharge occurred after 1945, and the presence of CFC-113 indicates that recharge occurred after 1965 (Bartolino 1997). The "Montreal Protocol on Substances that Deplete the Ozone Layer" was established in 1996 to stop CFC production in industrialized countries (Plummer and

Friedman, 1999). Since then, CFC concentrations in the atmosphere have leveled off or slightly declined (Plummer and Friedman 1999). Groundwater age is estimated from CFC data by comparing concentrations of CFCs in groundwater to the historical atmospheric concentrations of CFCs. As with most chemical tracers, biochemical processes can influence the concentrations of CFCs in groundwater. For instance, CFCs, particularly CFC-11, may be lost because of microbial degradation, leading to an older estimate of age. Other assumptions and factors that can affect the interpreted age include the temperature of the water table during recharge, the thickness of the unsaturated zone, the entrapment of excess air, uncertainty of recharge elevation, and the mixing of younger and older water in the aquifer (Plummer and Friedman, 1999). Introduction of atmospheric air during sampling will produce a younger CFC model date. Sampling methods for this study were designed so that there was little to no introduction of atmospheric air during sampling.

Carbon-14 is created in the upper atmosphere when cosmic rays interact with atmospheric nitrogen (Robertson et al. 2016). With a half-life of 5,730 years, carbon-14 can be useful to identify the age of water in an age range not covered by the other techniques used in this study.

Groundwater Travel Time (^{3}H and CFC)

Age differences from age dating of groundwater samples (Table S2) can be used to infer travel times if flow paths can be delineated. Groundwater in the alluvium valley between well Q and MV flows longitudinally (northeast to southwest) along the west part of the valley from well Q (upgradient) to MV (downgradient). While groundwater flow is three dimensional, in its simplest form it can be approximated as one dimensional.

A one-dimensional rate of groundwater velocity was calculated of approximately 1 ft/d (feet/day) from age differences in tracer data of ^{3}H between wells Q (upgradient) and MV (downgradient) and a linear distance calculated from x and y coordinates of the wells. A minimum age difference from ^{3}H of 27 years is likely given that well MV had an age of at least 60 years from 2016 (sample date) and well Q had an age date of 33 years from 2016. The difference in time over the linear distance equals approximately 27 years/9,835 feet or 1 ft/d. Graphically the time and distance is represented as a sloping line in Figure S5. Representing time distance as a linear line assumes that negligible recharge from the land surface (either precipitation and surface runoff) or negligible upwelling occurs from the Chinle between the two wells.

Well DD, which is located between Q and MV, had a ^{3}H date younger than well Q (Figure S5). We hypothesize this to be the result of mixing of dissolved gases from Chinle waters such as helium that can affect age calculations for ^{3}H. The average CFC age for CFC-11 and CFC-113 was 1976 at well DD. The projected line for age at that location is 1973 (difference of 3 years).

To confirm the reasonableness of one-dimensional travel times, a simple substitution into the one-dimensional Darcy equation (eq1) can be done to check the horizontal hydraulic conductivity (HK) of the alluvium.

Velocity = travel time = HK*I/ne (1)

where ne = equivalent porosity=0.25,

I = hydraulic gradient (Head difference between well Q and MV) divided by distance = 0.0048 ft/ft,

HK = horizontal (longitudinal) hydraulic conductivity,

Head difference = 6,551.52- 6,504.68, measured in May, 2016. Q head = 6551.52 ft and MV head = 6504.68 ft,

Distance = 9,835 FT (USED X,Y CORDINATES)

Inaccuracies in use of Equation 1 include time-varying hydraulic gradients, one-dimensional approximation to flow, assumption of a homogeneous and isotropic alluvium, and assumption of a uniform porosity. Using current hydraulic-head measurements to calculate hydraulic gradients may not be representative of historical gradients.

Solving (eq 1) for HK yields a bulk value of 52 ft/d. The average HK from solution of the steady-state radial flow equation and single well pump analysis using methods described by Harte (2017) is 9.5 ft/d for the 6 alluvial wells with hydraulic data from sampling of the wells. While a 5-fold difference in HK results, a solution within an order of magnitude is considered reasonable given that heterogeneity within the alluvium can cause preferential transport and quicker flows. Based on the average HK from the single well test (lower value than the travel time estimate), it suggests the potential for some younger waters mixing into the alluvium between wells Q and MV; otherwise, the time of travel would be longer based on the lower estimate of HK from single-well pump tests.

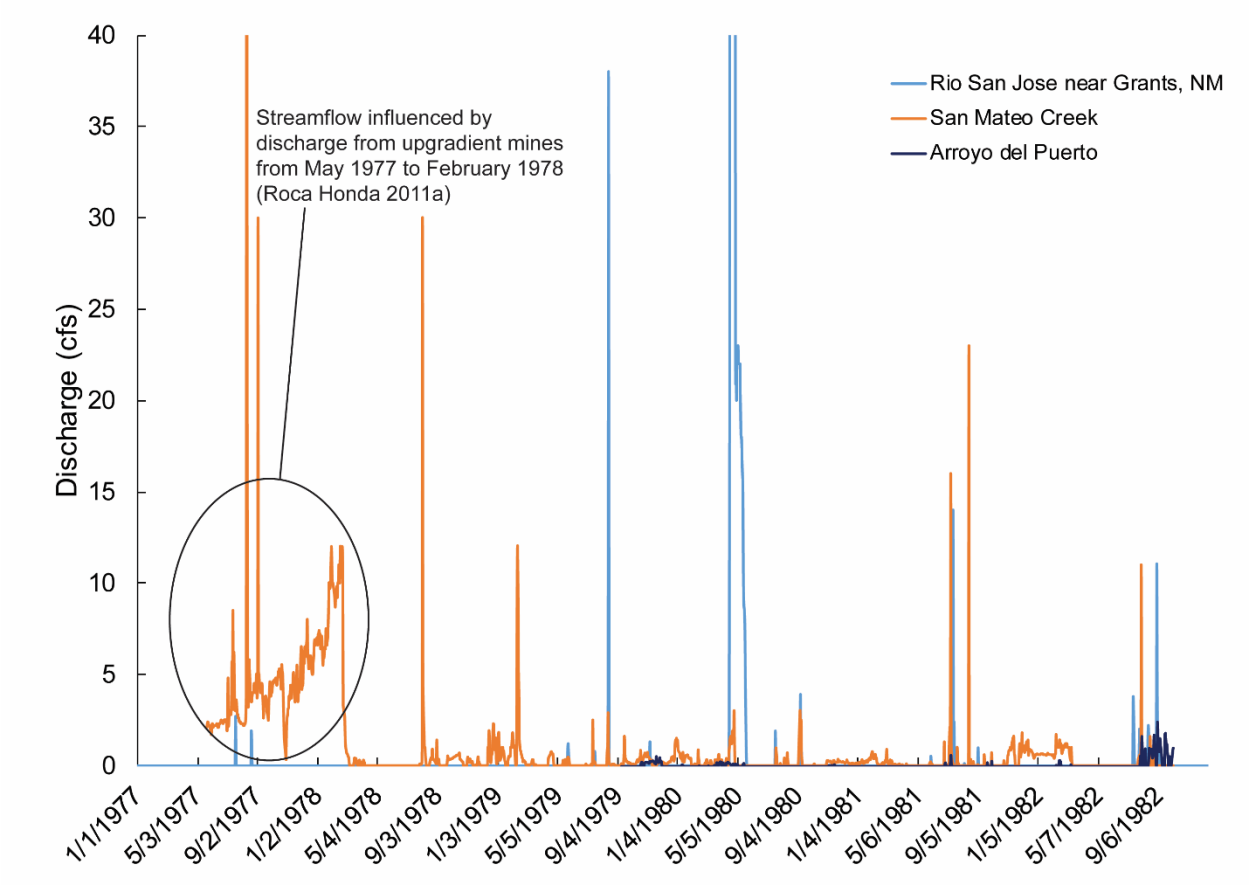

Figure S1. Discharge from USGS streamgaging stations for Rio San Jose near Grants, NM (USGS 0834300), San Mateo Creek nr San Mateo, NM (08342600), and Arroyo del Puerto nr San Mateo, NM (USGS 08342700). (cfs; cubic feet per second)

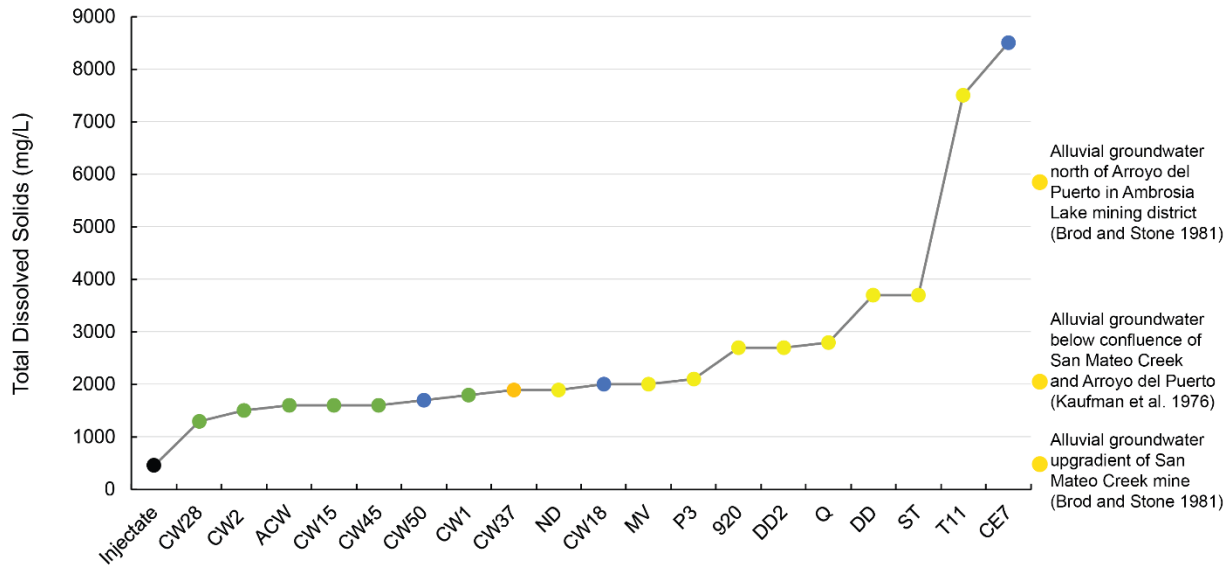

Figure S2. Total dissolved solids of water from alluvial and Chinle Group wells. Concentrations of total dissolved solids from alluvial groundwater upgradient of the Site are shown. (mg/L; milligrams per liter). Yellow circles are alluvial wells, green circles are Middle Chinle Group wells, orange circles are Upper Chinle Group wells, and the black circle is the Injectate..

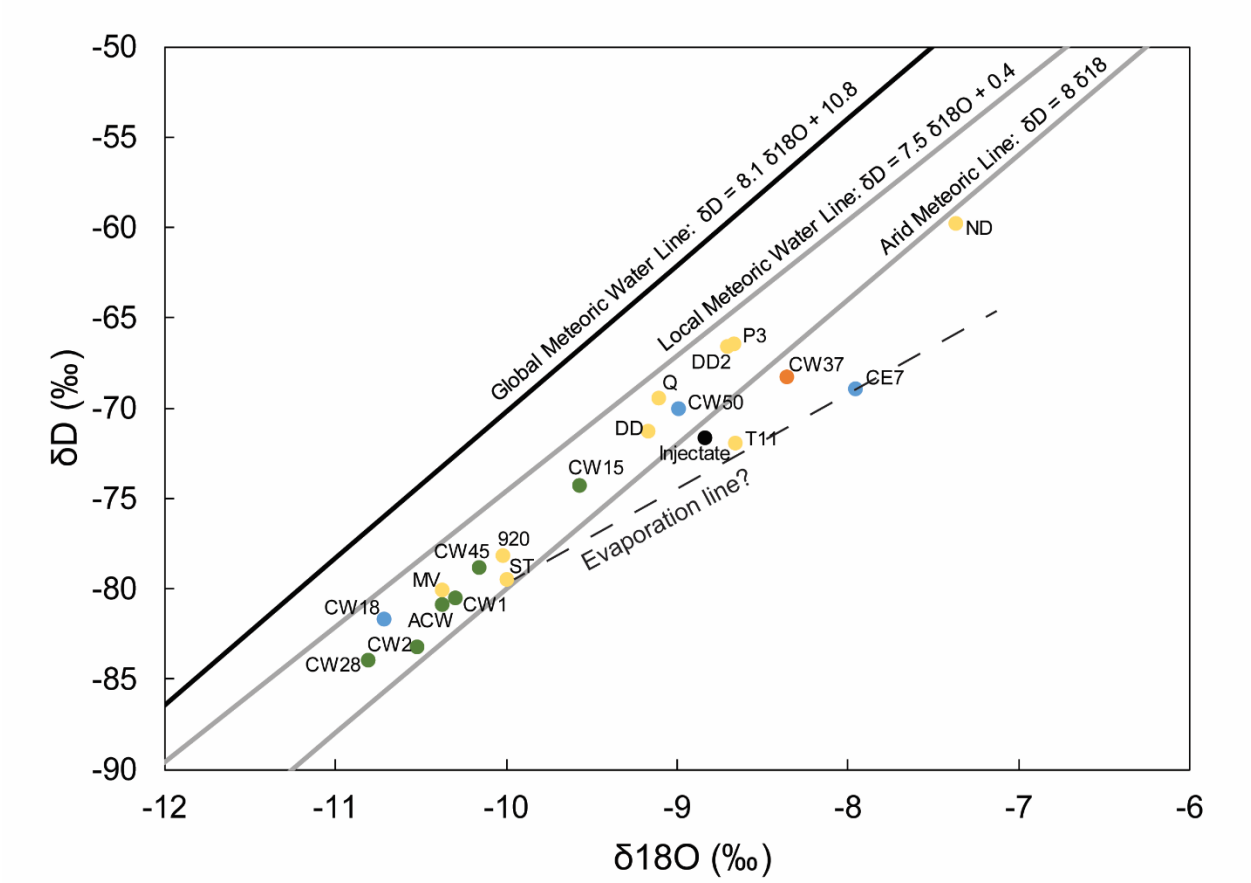

Figure S3. Plot of stable isotopes of water (δD and $\delta^{18}O$). The global meteoric water line, local meteoric line, and arid meteoric line are shown (Robertson et al. 2016). A potential evaporation line is plotted with a dashed line. (δD; deuterium; $\delta^{18}O$, oxygen 18; ‰, per mil in parts per thousand enrichments or depletions relative to a standard of known composition Yellow circles are alluvial wells, green circles are Middle Chinle Group wells, orange circles are Upper Chinle Group wells, and the black circle is the Injectate.

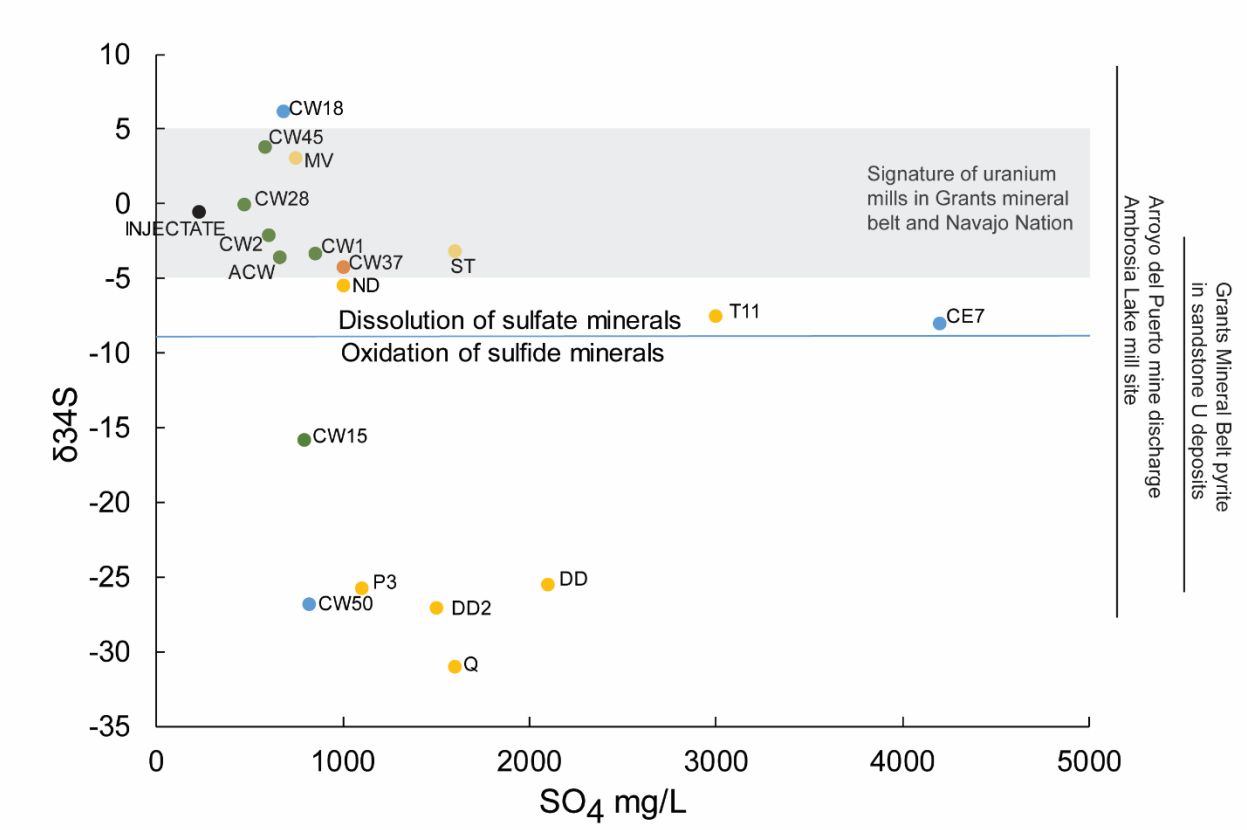

Figure S4. Plot of δ34S vs. SO_4. Known δ34S ranges are shown. (δ34S, sulfur 34 isotope in per mil; mg/L, milligrams per liter). Yellow circles are alluvial wells, green circles are Middle Chinle Group wells, orange circles are Upper Chinle Group wells, and the black circle is the Injectate.

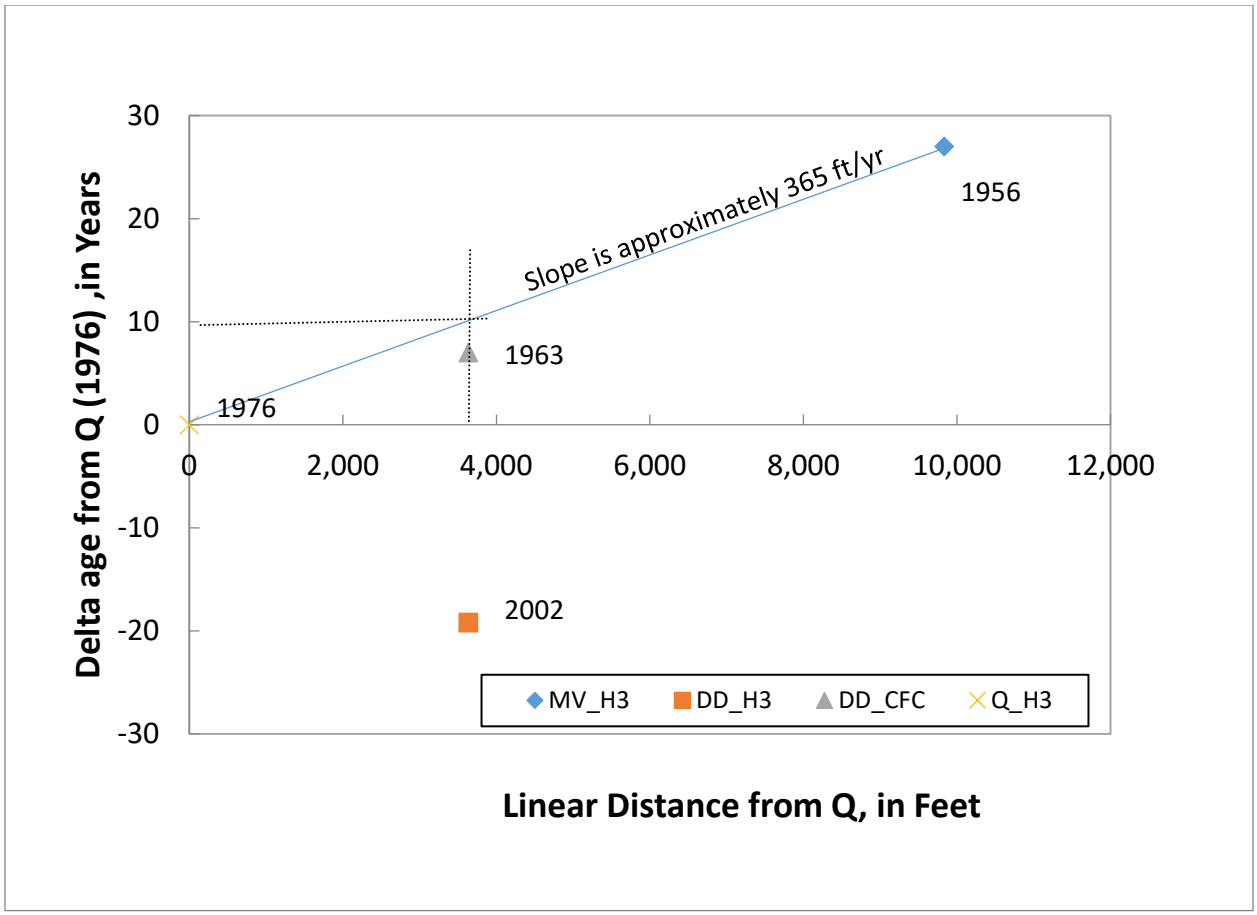

Figure S5. The time and distance from Well Q shown graphically as a sloping line. (Well Q is located at 0 distance)

Table S2. Modeled age dating results for tritium (^{3}H) and chloroflourocarbons (CFC). Modeled ages calculated as described by Plummer and Friedman (1999).

	Tritium				CFC			C-14			
Sample ID	Tritium Units	1-sigma error +/-	Calculated_Age(yr)_Ne_only_model	Calculated_Age(yr)_EA_model	Sample ID	CFC-11_Recharge_year	CFC-12_Recharge_year	CFC-113_Recharge_year	Sample ID	Type	Fraction Modern	Fraction Modern error
CW15	0.25	0.12	>60	>60	CW2	1952.5	1978	1970	P3	DIC	0.7271	0.0015
CW18	0.53	0.05	>60	>60	CW2	1950	1976.5	1943	DD2	DIC	0.4041	0.0011
CW37	2.21	0.20	not reporting/poor fit	not reporting/poor fit	CW2	1951.5	1978	1966				
DD	5.75	0.23	13.79	14.07	CW2 Rep	1948.5	1977	1943				
CW50	0.46	0.03	39.06	43.5	CW2 Rep	1950	1978	1943				
Q	3.23	0.15	33.08	35.2	CW2 Rep	1950.5	1975.5	1943				
MV	0.64	0.03	>60	>60	CW50 Rep	1950	1967	1970				
CW2	0.09	0.05	>60	>60	CW50 Rep	1947.5	1953.5	1958.5				
CW2 - Replicate	0.01	0.01	>60	>60	CW50 Rep	1953	1955	1943				
ND	0.77	0.10	-25.15	2.24	CW50	1951	1954.5	1943				
DD - Replicate	5.90	0.37	not reporting/poor fit	not reporting/poor fit	CW50	1956	1963.5	1969.5				
CW50 Replicate	–	–	no data	no data	CW50	1951	1955	1943				
T11	–	–	no data	no data	CW15	1958	#N/A	1971				
Injectate	–	–	no data	no data	CW15	1956.5	1966	1969.5				
					CW15	1961	1967	1973				
					DD	1970.5	#N/A	1981.5				
					DD	1971	#N/A	1982.5				
					DD	1970.5	#N/A	1980				
					Homestake	1963.5	1971.5	1967.5				
					Homestake	1967.5	#N/A	1972				
					Homestake	1966	1971	1972.5				
					DD Rep	1969.5	#N/A	1981				
					DD Rep	1970	#N/A	1979.5				
					DD Rep	1969	#N/A	1978.5				
					ND	1975	1976	1983.5				
					ND	1975.5	#N/A	1985.5				
					ND	1974	1981.5	1985				

References

Bartolino JR (1997) Chlorofluorocarbon and tritium age determination of ground-water recharge in the Ryan Flat subbasin, Trans-Peco Texas. U.S. Geological Survey Water-Resources Investigations Report 96-4245. 29 p.

Basu A, Brown ST, Christensen JN, DePaolo DJ, Reimus PW, Heikoop JM, Woldegabriel G, Simmons AM, House BM, Hartmann M, Maher K (2015) Isotopic and geochemical tracers for U(VI) reduction and U mobility at an in-situ recovery U mine. Environ Sci Technol, 49(10), 5939-5947. http://dx.doi.org/10.1021/acs.est.5b00701

Blake JMT, Becher KD, Harte PT, Thomas JV, Stengel VG (2017b) Data associated with uranium background concentrations at Homestake Mining Company Superfund Site, near Milan, New Mexico, July 2016 through October 2016 (ver. 1.1, August 2017). U.S. Geological Survey data release, https://doi.org/10.5066/F7CR5RJS.

Brod RC and Stone WJ (1981) Hydrogeology of Ambrosia Lake-San Mateo area, McKinley and Cibola Counties, New Mexico. New Mexico Bureau of Mines and Mineral Resources Hydrogeologic Sheet 2.

Buttigieg PL, Ramette A (2014) A guide to statistical analysis in microbial ecology—A community-focused, living review of multivariate data analyses. FEMS Microbiol Ecol, 90: 543–550.

Coplen, T.B., Qi, Haiping, Révész, Kinga, Casciotti, Karen, and Hannon, J.E., 2012, Determination of the $\delta^{15}N$ and $\delta^{18}O$ of nitrate in water; RSIL lab code 2900, chap. 17 *of* Stable isotope-ratio methods, sec. C *of* Révész, Kinga, and Coplen, T.B. eds., Methods of the Reston Stable Isotope Laboratory (slightly revised from version 1.0

released in 2007): U.S. Geological Survey Techniques and Methods, book 10, 35 p., available only at https://pubs.usgs.gov/tm/2006/tm10c17/

Harte PT (2017) In-well time-of-travel approach to evaluate optimal purge duration during low-flow sampling of monitoring wells. Environ Earth Sci, 76: 251. https://doi.org/10.1007/s12665-017-6561-5

Harte PT, Blake, JM, and Becher KD, (2018) Determination of representative uranium and selenium concentrations from groundwater, 2016, Homestake Mining Company Superfund site, Milan, New Mexico: U.S. Geological Survey Open-File Report 2018–1055, 40 p., appendixes, https://doi.org/10.3133/ofr20181055

Jiang Y, Guo H, Jia Y, Cao Y, Hu C (2015) Principal component analysis and hierarchical cluster analyses of arsenic groundwater geochemistry in the Hetao basin, Inner Mongolia. Chemie der Erde, 75: 197-205.

Kamp SD, Morrison SJ (2014) Use of chemical and isotopic signatures to distinguish between uranium mill-related and naturally occurring groundwater constituents. Ground Water Monit R, 34(1), 68–78. https://doi.org/10.1111/gwmr.12042.

Karim A, Veizer J (2000) Weathering processes in the Indus River Basin: implications from riverine carbon, sulfur, oxygen and strontium isotopes. Chem Geol, 170, 153-157.

Kaufman RF, Eadie GG, Russel, CR (1976) Effects of uranium mining and milling on groundwater in the Grants Mineral Belt, New Mexico. Ground Water, 14(5), 296-308. https://info.ngwa.org/GWOL/pdf/762502233.pdf.

Kimball, BA, Runkel, RL, Cleasby, TE, and Nimick, DA (2004) Quantification of metal loading by tracer injection and synoptic sampling, 1997-1998. Chapter D6 in Integrated investigations of environmental effects of historical mining in the basin

and Boulder mining districts, Boulder River watershed, Jefferson County, Montana. U.S. Geological Survey Professional Paper 1652-D6.

Landa E (1980) Isolation of uranium mill tailings and their component radionuclides from the biosphere-Some Earth science perspectives. U.S. Geological Survey Circular 814.

Langman JB, Sprague JE, Durall RA (2012) Geologic framework, regional aquifer properties (1940s-2009), and spring, creek and seep properties (2009-10) of the Upper San Mateo Creek Basin near Mount Taylor, New Mexico. U.S. Geological Survey Scientific Investigations Report 2012-5019, 96.

Lee L (2015) Package 'NADA', Nondetects and data analysis for environmental data, version 1.5-6: The Comprehensive R Archive Network web page, accessed December 2017, at https://cran.r-project.org/web/packages/NADA/NADA.pdf

Lucas LL, Unterweger PM (2000) Comprehensive review and critical evaluation of the half-life of tritium. Journal of Research of the National Institute of Standards and Technology, 105, https://doi.org/10.6028/jres.105.043.

New Mexico Environment Department (NMED), 2012, Site inspection report, Phase 2, San Mateo Creek Basin legacy uranium mine and mill site area, CERCLIS ID NMN000606847, Cibola-McKinley Counties, New Mexico, https://www.epa.gov/sites/production/files/2015-05/documents/san_mateo_creek_si_phase_2-report_final.pdf

Nuclear Regulatory Commission, 1981, Appendix A- Report on Alkaline carbonate leaching at Homestake Mining Company, https://www.nrc.gov/docs/ML0702/ML070240368.pdf Accessed 16 June 2018

Oksanen J, Guillaume Blanchet F, Friendly M, Kindt R, Legendre P, McGlinn D, Minchin PR, O'Hara RB, Simpson GL, Solymos P, Henry M, Stevens H, Szoecs E, Wagner H (2016) Package 'vegan': The Comprehensive R Archive Network web page, Community ecology package, version 2.4-1, accessed December 2017, at https:// cran.r-project.org/web/packages/vegan/index.html.

Plummer NL, Friedman LC (1999) Tracing and dating young ground water. U.S. Geological Survey Fact Sheet 134-99, 4 pp.

Ries KS (1982) Stable oxygen and sulfur isotopes applied to tracing seepage from mine tailings. Master's Thesis, The University of Arizona, http://hdl.handle.net/10150/191770 Accessed 12 February 2018

Révész K, Coplen TB (2008) Determination of the $\delta(^{18}O/^{16}O)$ of water: RSIL lab code 489, chap. C2 of Révész, Kinga, and Coplen, Tyler B., eds., Methods of the Reston Stable Isotope Laboratory. U.S. Geological Survey Techniques and Methods, 10–C2, 28 p.

Révész, Kinga, Qi, Haiping, and Coplen, T.B., 2012, Determination of the $\delta^{34}S$ of low-concentration sulfate in water; RSIL lab code 1949, chap. 8 *of* Stable isotope-ratio methods, sec. C *of* Révész, Kinga, and Coplen, T.B. eds., Methods of the Reston Stable Isotope Laboratory (slightly revised from version 1.1 released in 2007): U.S. Geological Survey Techniques and Methods, book 10, 35 p., available only at https://pubs.usgs.gov/tm/2006/tm10c8/. (Supersedes versions 1.0 Robertson AJ, Ranalli AJ, Austin SA, Lawlis BR (2016) The source of groundwater and solutes to Many Devils Wash at a former uranium mill site in Shiprock, New Mexico. U.S. Geological Survey Scientific Investigations Report 2016–5031, 54 p., http://dx.doi.org/10.3133/sir20165031.

SigmaPlot (2018) version 14.0, from Systat Software, Inc., San Jose California USA, www.systatsoftware.com.